

# Theory of Triplet Optical Absorption in Oligoacenes: From Naphthalene to Heptacene

Himanshu Chakraborty and Alok Shukla

*Department of Physics, Indian Institute of  
Technology Bombay, Powai, Mumbai 400076, INDIA\**

## Abstract

In this paper we present a detailed theory of the triplet states of oligoacenes containing up to seven rings, *i.e.*, starting from naphthalene all the way up to heptacene. In particular, we present results on the optical absorption from the first triplet excited state  $1^3B_{2u}^+$  of these oligomers, computed using the Pariser-Parr-Pople (PPP) model Hamiltonian, and a correlated electron approach employing the configuration-interaction (CI) methodology at various levels. Excitation energies of various triplets states obtained by our calculations are in good agreement with the experimental results, where available. The computed triplet spectra of oligoacenes exhibits rich structure dominated by two absorption peaks of high intensities, which are well separated in energy, and are caused by photons polarized along the conjugation direction. This prediction of ours can be tested in future experiments performed on oriented samples of oligoacenes.

---

\* [chakraborty.himanshu@gmail.com](mailto:chakraborty.himanshu@gmail.com), [shukla@phy.iitb.ac.in](mailto:shukla@phy.iitb.ac.in)

## I. INTRODUCTION

Conjugated polymers form a class of materials which are strong candidates for building the next generation of optoelectronic devices.<sup>1,2</sup> In order to be able utilize them for these purposes, a thorough understanding of their electronic structure and optical properties is essential. Most of the polymers useful for optoelectronic devices have singlet ground states, and, therefore, singlet excited states determine their optical properties. As a result of that, most of the theoretical studies of optical properties of conjugated polymers, have concentrated on the absorption spectra in the singlet manifold.<sup>3</sup> However, the triplet states of these systems have become important because of the possibility of “singlet fission”, *i.e.*, a singlet excited state decaying into two triplets leading to higher photo voltaic yield.<sup>4,5</sup> Furthermore, within the tight-binding model, the lowest triplet state has the same orbital occupancy and spatial symmetry as the lowest optically active singlet state, thus rendering them degenerate. Therefore, differences between these two states will be due to electron correlation effects, and, thus, a study of triplet states provides us with an insight into the role of electron correlations in that material.<sup>6</sup>

Recently, polyacenes have been considered as strong candidates for optoelectronic device applications such as light-emitting diodes, and field effect transistors.<sup>7–10</sup> Furthermore, because of their structural similarities to zigzag graphene nanoribbons,<sup>7,11</sup> the research effort involving various oligoacenes has further intensified. Although, most of the studies have concentrated on oligoacenes ranging from naphthalene to pentacene, several recent works have reported the synthesis of longer oligomers such as hexacene, heptacene, and beyond.<sup>12–15</sup> Over the years, optical properties of oligoacenes have been studied extensively, however, most of these studies have been confined to their ground state absorption into higher singlet states,<sup>7,8,16</sup> with the number of studies dedicated to triplet states being far fewer. Triplet states of naphthalene have been probed experimentally by Lewis *et al.*,<sup>17</sup> McClure,<sup>18</sup> Hunziker,<sup>19,20</sup> and Meyer *et al.*<sup>21</sup> Similarly, experimental measurements of the triplet states in longer stable oligomers namely anthracene,<sup>21–24</sup> tetracene,<sup>21–23,25–27</sup> and pentacene,<sup>27–29</sup> have also been performed. A few triplet state measurements of relatively unstable hexacene,<sup>30</sup> and heptacene<sup>12</sup> also exist. Recently, several experimental measurements of the triplet states have also been performed on thin films, crystalline, and dimeric samples of tetracene<sup>31,32</sup> and pentacene,<sup>32–37</sup> predicting that the lowest triplet state is of charge transfer type.

As far as theoretical studies of the triplet states of oligoacenes are concerned, using a Pariser-Parr-Pople (PPP) model type semi-empirical approach,<sup>38,39</sup> early calculations were performed by Pariser.<sup>40</sup> Subsequently, again using the PPP model, low-order configuration interaction (CI) calculations of triplet states of various oligoacenes were performed by Groot and Hoytink,<sup>41</sup> and Angliker *et al.*<sup>30</sup> A self-consistent-field random-phase-approximation (SCF-RPA) scheme also within the PPP model was employed by Baldo *et al.*<sup>42</sup> to perform calculations of triplet states in polyacenes. Large scale density matrix renormalization group (DMRG) based calculations using the PPP model, have been performed by Ramasesha and co-workers,<sup>43</sup> and recently, they reported exact diagonalization (full CI) calculations, for tetracene.<sup>44</sup> Complete neglect of differential overlap (CNDO) based CI calculations employing CNDO/S2 parameterization were done by Lipari and Duke,<sup>45</sup> while CNDO/S-CI method was used by Sanche and co-workers<sup>46</sup> for triplet excited state calculations. Gao *et al.*<sup>47</sup> employed a spin Hamiltonian and valence bond approach to compute the triplet states of oligoacenes. As far as *ab initio* calculations are concerned, complete-active-space self-consistent field (CASSCF) and perturbation theory (PT2F) calculations on these systems were performed by Rubio *et al.*,<sup>48</sup> while multi-reference Møller-Plesset (MRMP) theory calculations were reported by Hirao and co-workers,<sup>49,50</sup> and Zimmerman *et al.*<sup>51</sup> Chan and co-workers<sup>52</sup> reported calculations of triplet states of oligoacenes combining the CASSCF and density-matrix renormalization group (DMRG) approaches, while coupled-cluster theory (CCSD(T)) based calculations were performed by Hajgato *et al.*<sup>53</sup> Numerous first-principles density-functional theory (DFT) based calculations have also been performed by various authors which include works of Houk *et al.*,<sup>54</sup> Quarti *et al.*,<sup>55</sup> Anger and co-workers,<sup>33</sup> Hummer *et al.*,<sup>56</sup> Bendikov *et al.*,<sup>7</sup> Nguyen *et al.*,<sup>57</sup> and spin-polarized DFT calculations by Jiang and Dai.<sup>58</sup> Most of the theoretical studies mentioned above either concentrated on a class of triplet excited states of small oligomers, or only on the energetics of their lowest triplet excited state. However, none of the earlier works have reported the calculations of triplet optical absorption spectra, which involves not only the energetics and the wave functions of a number of triplet excited states, but also computation of their transition dipole moments with respect to the lowest triplet state.

In this work, we have performed large-scale correlated electron calculations of optical absorption in the triplet manifolds of oligoacenes ranging from naphthalene up to heptacene, using the multi-reference singles-doubles CI (MRSDCI) method, employing the PPP model

Hamiltonian. The detailed results obtained for the low-lying triplet excited states of these acenes are presented and compared with different experimental and other theoretical works. Our calculated energies of the lowest triplet excited states,  $1^3B_{2u}^+$ ,  $1^3B_{1g}^-$ ,  $1^3B_{1g}^+$ ,  $1^3A_g^-$ , and  $1^3A_g^+$  for these oligoacenes show very good agreement with the experimental results. The calculated triplet absorption spectra of these oligoacenes reveal two long-axis polarized intense peaks which are well separated in energy, as against one intense peak observed in their singlet absorption spectra. This observation is in agreement with our earlier triplet absorption calculations of the longer acenes namely octacene, nonacene and decacene,<sup>59</sup> and can be tested in future experiments on the oriented samples of oligoacenes.

Remainder of this paper is organized as follows. In the section II we describe the theoretical methodology employed for performing these calculations. Then, in section III, we present and discuss our results. Finally, in section IV, we present our concluding remarks, while the convergence of lowest triplet excitation energies with respect to the PPP parameters, influence of geometry on the triplet energies, and the convergence of the MRSDCI excitation energies along with the quantitative details of the excited states contributing to the absorption spectra, and their many-particle wave functions, are presented in the Appendixes A and B.

## II. THEORY

Fig.1 presents the schematic structure of an oligocene lying in the  $xy$ -plane, where the  $x$ -axis is assumed to be the conjugation direction. For the purpose of computational simplicity, a highly symmetric geometry of oligoacenes has been employed in these calculations, with all nearest-neighbor carbon-carbon bond lengths fixed at 1.4 Å, and all the bond angles assumed to be 120°. However, explicit calculations have been performed, in Appendix A, to demonstrate that the triplet optical absorption spectra obtained using realistic asymmetric geometries, with non-uniform bond lengths and bond angles, do not exhibit any significant differences as compared to the symmetric geometry adopted in the present work.

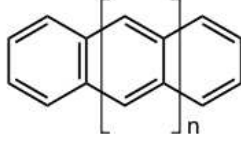


Figure 1. Schematic drawings of polyacenes

The symmetric structure can be viewed as two identical polyene chains of suitable lengths, coupled along the  $y$ -direction. We have used the PPP model Hamiltonian<sup>38,39</sup> for the correlated calculations, which can be decomposed as

$$H = H_{C_1} + H_{C_2} + H_{C_1C_2} + H_{ee},$$

where the first two terms,  $H_{C_1}$  and  $H_{C_2}$  depict the one-electron Hamiltonians for the carbon atoms located on the upper and the lower polyene like chains, respectively. The third term,  $H_{C_1C_2}$  is the one-electron hopping between the two chains, and the last term,  $H_{ee}$  represents the electron-electron repulsion. The individual terms can be written as follows in the second-quantized notation,

$$H_{C_1} = -t_0 \sum_{\langle k, k' \rangle} B_{k, k'},$$

$$H_{C_2} = -t_0 \sum_{\langle \mu, \nu \rangle} B_{\mu, \nu},$$

$$H_{C_1C_2} = -t_{\perp} \sum_{\langle k, \mu \rangle} B_{k, \mu}.$$

$$H_{ee} = U \sum_i n_{i\uparrow} n_{i\downarrow} + \frac{1}{2} \sum_{i \neq j} V_{i,j} (n_i - 1)(n_j - 1)$$

In the equation above, the carbon atoms on the upper and lower polyene chains are denoted by  $k$ ,  $k'$  and  $\mu, \nu$  respectively, whereas  $i$  and  $j$  depict all the atoms of the oligomer. The nearest neighbors are represented by the symbol  $\langle \dots \rangle$ , and  $B_{i,j} = \sum_{\sigma} (c_{i,\sigma}^{\dagger} c_{j,\sigma} + h.c.)$ , where

$h.c.$  denotes the Hermitian conjugate. The one-electron hops are denoted by the matrix elements  $t_0$ , and  $t_\perp$ . We took the quantitative value of the hopping matrix elements as  $t_0 = 2.4$  eV for both intracell and intercell hoppings, and  $t_\perp = t_0$ , in agreement with the undimerized ground state for polyacene asserted by Raghu *et. al.*<sup>43</sup>

The Coulomb interactions are parametrized according to the Ohno relationship,<sup>60</sup>

$$V_{i,j} = U/\kappa_{i,j}(1 + 0.6117R_{i,j}^2)^{1/2} ,$$

where,  $\kappa_{i,j}$  denotes the dielectric constant of the system to reproduce the effects of screening. The on-site repulsion term is depicted by  $U$ , while  $R_{i,j}$  implies the distance in Å between the  $i$ th carbon and the  $j$ th carbon. The present calculations have been carried out using: (a) “standard parameters”<sup>60</sup> with  $U = 11.13$  eV and  $\kappa_{i,j} = 1.0$ , and (b) “screened parameters”<sup>61</sup> with  $U = 8.0$  eV and  $\kappa_{i,j} = 2.0$  ( $i \neq j$ ) and  $\kappa_{i,i} = 1.0$ . Chandross and Mazumdar,<sup>61</sup> devised the screened parameters, so as to account for the inter-chain screening effects in phenylene based polymers. However, they can also be seen to describe the effect of the host in solution or thin-film based experiments. In Appendix A 1, we examine the effect of variations in the values of various PPP parameters, on the computed excitation energy of the lowest triplet state of naphthalene.

Several authors compute high-spin states such as the triplet state using broken symmetry unrestricted HF (UHF) approach, or its DFT counterpart unrestricted DFT (UDFT) methods.<sup>54,58,62</sup> Although such wave functions have  $z$ -component of the total spin ( $S_z$ ) as a good quantum number, but they are not eigenstates of the total spin ( $S^2$ ). Such calculations normally lead to results which can be seen as artifacts of the method because of the large spin contamination associated with the corresponding many-particle wave functions.<sup>53,63,64</sup> Therefore, in this work we use only the restricted HF method (RHF), coupled with the CI approach where the many-particle wave function is an eigenfunction of both  $S^2$  and  $S_z$  operators, in addition to the corresponding point group operators. Thus our calculations are initiated by performing RHF calculations, employing the PPP Hamiltonian, using a computer code developed in our group.<sup>65</sup> All the resultant HF molecular orbitals are treated as active orbitals. For shorter acenes, full configuration interaction (FCI) method was used, while for the longer ones quadruple CI (QCI) and MRSDCI methods were employed. In particular, FCI method was used for naphthalene and anthracene, while the QCI/MRSDCI methods

were employed from tetracene onwards. The MRSDCI method,<sup>66,67</sup> is a well known technique which includes electron-correlation effects beyond the mean-field both for the ground and excited states of molecular systems. In this approach, the CI matrix is constructed by generating singly and doubly excited configurations with respect to a given set of reference configurations which are specific to the states being targeted in the calculation. The calculations are performed in an iterative manner until acceptable convergence has been achieved. We have used this methodology extensively within the PPP model to study the optical properties of a number of conjugated polymers,<sup>6,16,59,68–70</sup> and refer the reader to those papers for the technical details associated with the approach.

### III. RESULTS AND DISCUSSIONS

Table I. Total number of orbitals of different symmetries used in our calculations, for oligoacenes (acene- $n$ ) of increasing length,  $n$ . Both the standard and screened parameters have the same number of orbitals for the mentioned symmetries. The number in the parenthesis for each symmetry indicates the number of doubly-occupied orbitals of that symmetry in the Hartree-Fock ground state. The number of unoccupied orbitals of a given symmetry can be obtained simply by subtracting the number of occupied orbitals of that symmetry, from the total number of orbitals of the symmetry concerned.

$n$	$A_g$	$B_{2u}$	$B_{3u}$	$B_{1g}$
2	3(2)	3(1)	2(1)	2(1)
3	4(2)	4(2)	3(2)	3(1)
4	5(3)	5(2)	4(2)	4(2)
5	6(3)	6(3)	5(3)	5(2)
6	7(4)	7(3)	6(3)	6(3)
7	8(4)	8(4)	7(4)	7(3)

Table II. The sizes of the CI matrix diagonalized, for different symmetries of oligoacenes (acene- $n$ ) of increasing length,  $n$ . Below std and scr refer to standard and screened parameters, respectively. Superscripts  $a$ ,  $b$ ,  $\dots$  etc. refer to the type of CI calculations performed, and are explained below.

$n$	$^1A_g^-$	$^1B_{2u}^+$	$^3B_{2u}^+$	$^3A_g^-$	$^3B_{1g}^-$
2	4936 <sup>a</sup>	4794 <sup>a</sup>	7370 <sup>a</sup>	7360 <sup>a</sup>	7440 <sup>a</sup>
3	623576 <sup>a</sup>	618478 <sup>a</sup>	1099182 <sup>a</sup>	1106140 <sup>a</sup>	1104544 <sup>a</sup>
4	193538 <sup>b</sup>	335325 <sup>b</sup>	614865 <sup>b</sup>	201879 <sup>c</sup>	217203 <sup>c</sup>
				224735 <sup>c</sup>	224266 <sup>c</sup>
5	1002597 <sup>b</sup>	1707243 <sup>b</sup>	3202299 <sup>b</sup>	582278 <sup>c</sup>	490532 <sup>c</sup>
				621397 <sup>d</sup>	531551 <sup>d</sup>
6	3940254 <sup>b</sup>	6434183 <sup>b</sup>	12234931 <sup>b</sup>	1231948 <sup>c</sup>	1156916 <sup>c</sup>
				1443726 <sup>d</sup>	1107262 <sup>d</sup>
7	12703819 <sup>b</sup>	19663495 <sup>b</sup>	37724739 <sup>b</sup>	2414274 <sup>c</sup>	1848466 <sup>c</sup>
				2611198 <sup>d</sup>	1795626 <sup>d</sup>

<sup>a</sup>FCI

<sup>b</sup>QCI

<sup>c</sup>MRSDCI (std)

<sup>d</sup>MRSDCI (scr)

Before discussing our results, we present the total number of orbitals used for the different symmetries, in the Table I, while in Table II the dimensions of the CI matrices employed for calculating the ground and excited states of different symmetries, for oligoacenes of increasing lengths. We note that the largest QCI calculation performed on heptacene involved dimension in excess of thirty seven million configurations. Thus, given the large-scale nature of these calculations, we are confident that electron-correlation effects have been accounted for in an adequate manner. Because of the large dimensions of these matrices, typically lowest 50–70 of their eigenroots were computed using Davidson algorithm as implemented in the MELD program.<sup>71</sup> In spite of this restriction in the number of computed eigenvectors, the energy region covered for computing the absorption spectra was sufficiently large so as to allow comparison of our results with the experiments in a broad spectral range. For the calculations presented here, we have ensured that the convergence with respect to the size



of the CI expansion has been achieved, and in Appendix A, for the case of anthracene, we have demonstrated the convergence of the MRSDCI calculations by comparing them with the FCI result.

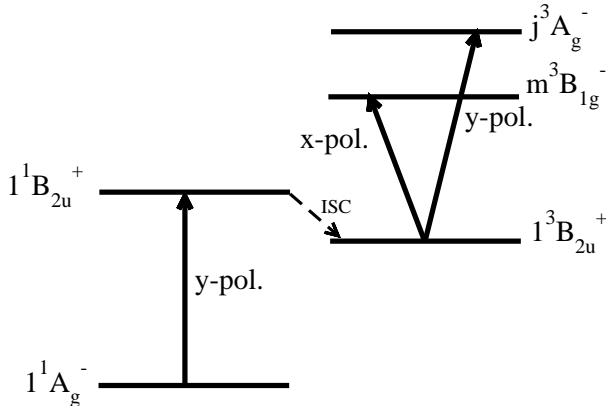


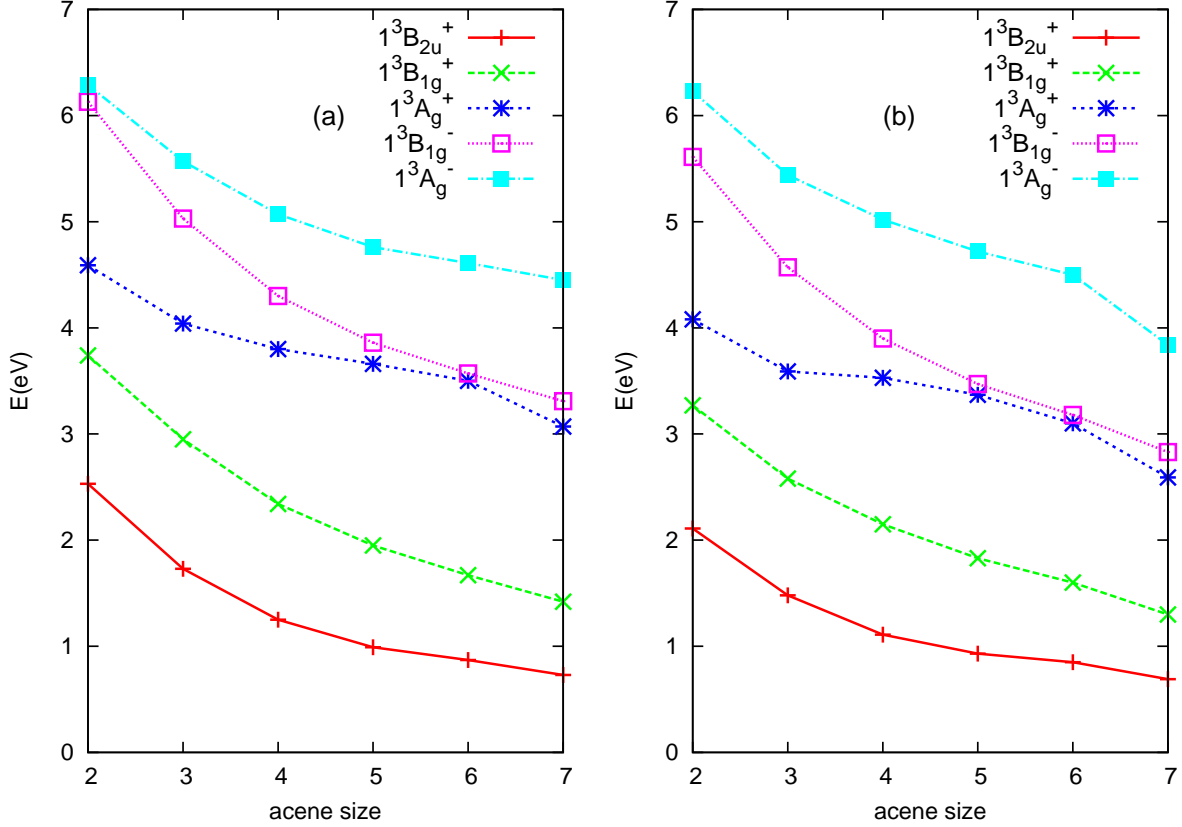
Figure 2. Diagram depicting the important states in the triplet excited state absorption in oligoacenes, along with their polarization characteristics. The optical absorption is denoted by the arrows connecting two states, and the polarization directions are denoted next to them. Inter-system crossing (ISC) is shown as dotted lines. Location of the states is not up to scale.

Triplet excited state absorption can be explained by means of a schematic diagram shown in Fig. 2. Light absorption takes place from  $1^3B_{2u}^+$  ( $T_1$ ) state through long-axis ( $x$ ) or short-axis ( $y$ ) polarized photons leading the system to  $^3B_{1g}^-$  or  $^3A_g^-$  type excited states. As far as the energetics of various excited states are concerned, our results are summarized in Tables III and IV, where experimental and theoretical results obtained by other authors are also presented. In triplet absorption experiments, the excitation energies are measured with respect to the reference  $1^3B_{2u}^+$  state. Therefore, to keep the comparison with the experiments transparent, in Tables III and IV we present the energies of  $^3B_{1g}^-$  or  $^3A_g^-$  type excited states with respect to the  $1^3B_{2u}^+$  state. However, excitation energies of these states with respect to the  $1^1A_g^-$  ground state are presented in various tables in Appendix B, as also in Fig. 3.

## A. Energies of Triplet States

Before discussing the cases of individual oligomers, first we make a few general comments about the results presented in Tables III and IV. Additionally, the plots of the excitation energies of the lowest excited triplet states of various symmetries, namely,  $1^3B_{2u}^+$ ,  $1^3B_{1g}^+$ ,  $1^3A_g^+$ ,  $1^3B_{1g}^-$  and  $1^3A_g^-$ , with respect to the ground state  $1^1A_g^-$ , as a function of the increasing acene size ( $n$ ) are presented in Figure 3. Before we discuss our results in detail, we would like to emphasize the fact that because PPP model does not take vibrational degrees of freedoms into account, our calculated values of excitation energies of various states are essentially “vertical excitation energies”. However, experimental measured values of the same quantities, depending upon the technique employed, may, or may not, be vertical values. Therefore, while comparing our results with the experimental ones in the following discussion, we also mention the experimental technique involved. We also have to bear in mind that one of the reasons behind the disagreement between the theory and the experiment could be the fact that the experiment in question may not be measuring the vertical excitation energies.

Figure 3. Variation of the excitation energies (with respect to the ground state,  $1^1A_g^-$ ) of the lowest excited triplet states of various symmetries, as a function of acene size ( $n$ ) calculated using: (a) standard parameters, and (b) screened parameters.



As far as the excitation energy of first triplet excited state  $1^3B_{2u}^+$  state is concerned, our standard parameter based results are in better agreement with the experiments as compared to the screened parameter ones, for naphthalene, anthracene and tetracene. From pentacene onwards, the results obtained with the two parameter sets tend to merge, however, experimental results are not available for the  $1^3B_{2u}^+$  state of heptacene.

Other important triplet states for oligoacenes are  $1^3B_{1g}^+$ ,  $1^3A_g^+$ ,  $1^3B_{1g}^-$ , and  $1^3A_g^-$ . Of these, optical transitions to  $1^3B_{1g}^+$  and  $1^3A_g^+$  from the  $1^3B_{2u}^+$  state are dipole forbidden within the PPP model, because of the particle-hole symmetry inherent in the system due to the nearest-neighbor hopping approximation. In reality, of course, particle-hole symmetry is

approximate, and, therefore, these states are faintly visible in the excited state absorption from the  $T_1$ . Even though in our calculations these states are absent in the computed spectra, nevertheless, it is possible to identify them by examining their many-particle wave functions.

Our calculated values of the excitation energies of the dipole forbidden state  $1^3B_{1g}^+$  obtained using both sets of Coulomb parameters are in good qualitative agreement with each other, although, quantitatively speaking, the standard parameter values are slightly larger than the screened parameter ones. As far as the experiments are concerned, the values of  $E(1^3B_{1g}^+) - E(1^3B_{2u}^+)$  are available only for naphthalene, anthracene, and tetracene, and in those cases our calculated results appear to be slightly lower than the experimental values. Similar trends hold for the other dipole forbidden state,  $1^3A_g^+$  as well, except that the standard parameter value of  $E(1^3A_g^+) - E(1^3B_{2u}^+)$  for tetracene is in excellent agreement with the experimental ones.

As far as the theoretical values of  $E(1^3A_g^+) - E(1^3B_{2u}^+)$ , an interesting trend emerges irrespective of the parameters used, in that with the increasing length of the oligomers up to pentacene, this excitation energy increases. Experimentally speaking, a similar trend is visible for all the oligomers up to tetracene, while for the longer oligomers, the experimental values are not available. This counterintuitive trend in the values of  $E(1^3A_g^+) - E(1^3B_{2u}^+)$ , with respect to the oligomer lengths, suggests that  $1^3A_g^+$  state is much more localized than the  $1^3B_{2u}^+$  state because of which the decrease in the value of  $E(1^3A_g^+)$ , with the increasing oligomer length, is slower as compared to  $E(1^3B_{2u}^+)$ . Therefore, it will be of tremendous interest to measure this value for longer acenes as well, so that this theoretical prediction of ours can be tested.

For the dipole allowed state  $1^3B_{1g}^-$ , the excitation energies computed by the standard parameters are larger than those computed by screened parameters for all the oligomers. Experimental values of these excitation energies are available for all the oligoacenes considered here, and, on the average, much better agreement is found with the screened parameter results.

For the  $1^3A_g^-$  state, however, screened parameter values of the excitation energies are larger compared to the standard ones for naphthalene, anthracene, and tetracene (*cf.* Table III), almost equal for pentacene, and smaller for hexacene and heptacene (*cf.* Table IV). Experimental values of  $E(1^3A_g^-) - E(1^3B_{2u}^+)$  are available up to pentacene, and, they have

disagreements amongst themselves for naphthalene and tetracene for which multiple values have been reported. Overall, the experimental results are in good agreement with the theory, except for the case of pentacene, for which theoretical values are larger than the measured one.

Next, we present a comparison of our results for individual oligomers with the theoretical works of other authors, as well as with the experiments.

### 1. Naphthalene

For naphthalene and anthracene FCI calculations have been performed which yield exact results within the chosen model Hamiltonian, and, therefore, cannot be improved. Thus, any discrepancy in the results with respect to the experiments has to be understood as a limitation of the PPP model, or the parameters used to describe it.

Since we have performed calculations on isolated oligomers, therefore, most appropriate comparison will be with the experiments performed in the gas or liquid solution phase.

Lewis and Kasha,<sup>17</sup> and McClure,<sup>18</sup> based upon their solution based experiments, on phosphorescence spectra observed in EPA at 90K and in rigid glass solution at liquid  $N_2$  temperature, respectively, reported the value of  $E(1^3B_{2u}^+)$  of naphthalene to be 2.64 eV. Exactly the same value was also reported by Swiderek *et al.*<sup>46</sup> based upon electron-energy loss spectroscopy measurements of naphthalene deposited on solid argon thin films. This value is in very good agreement with our standard parameter based value of 2.53 eV, but is significantly larger than the screened parameter value of 2.11 eV. As far as comparison with other theoretical works goes, our standard parameter value of  $E(1^3B_{2u}^+)$  is in almost perfect agreement with the PPP-FCI value of 2.52 eV reported by Ramasesha and Soos,<sup>73</sup> and in good agreement with the CCSDT(T) value of 2.72 eV reported by Hajgato *et al.*,<sup>53</sup> first-principles DMRG value of 2.67 eV reported by Hachmann *et al.*,<sup>52</sup> and 2.71 eV reported by Houk *et al.*,<sup>54</sup> computed using the B3LYP as exchange-correlation functional with a 6-31G\* basis sets. The value 3.11 eV reported by Thiel *et al.*,<sup>72</sup> for the excitation energy of the  $1^3B_{2u}^+$  state, computed using the coupled cluster method CC3, with TZVP basis set,

Table III. Comparison of results of our triplet calculations for naphthalene, anthracene, and tetracene, performed using the standard (std.)/screened (scr.) parameters in PPP model, with other experimental and theoretical results for the most important low-lying states. As explained in the text, energies of the excited states of  ${}^3B_{1g}$  and  ${}^3A_g$  type, are given with respect to the  $1^3B_{2u}^+$  state.

State			Excitation energy (eV)			
	Present work		Experimental		Other theoretical	
	std.	scr.				
Naphthalene (C <sub>10</sub> H <sub>8</sub> )						
$1^3B_{2u}^+$	2.53	2.11	2.64(l) <sup>17,18,46</sup>		3.11, <sup>72</sup> 2.52, <sup>73</sup> 2.72, <sup>53</sup> 2.18, <sup>40</sup> 2.71, <sup>54</sup> 2.67, <sup>52</sup> 2.98, <sup>46</sup> 3.05 <sup>48</sup>	
$1^3B_{1g}^+$	1.21	1.16	1.30-1.35(l) <sup>21</sup>		1.36, <sup>72</sup> 1.18, <sup>41</sup> 1.24, <sup>40</sup> 1.10, <sup>46</sup> 1.14 <sup>48</sup>	
$1^3A_g^+$	2.06	1.97	1.97(l), <sup>21</sup> 2.25(g) <sup>20</sup>		2.41, <sup>72</sup> 2.03, <sup>41</sup> 2.25, <sup>40</sup> 2.01, <sup>46</sup> 2.18 <sup>48</sup>	
$1^3B_{1g}^-$	3.60	3.50	3.12(g), <sup>19,23</sup> 2.98(l), <sup>26</sup> 3.00(l) <sup>21</sup>		3.29, <sup>41</sup> 3.52, <sup>40</sup> 3.24, <sup>46</sup> 2.61, <sup>48</sup> 2.71 <sup>49</sup>	
$1^3A_g^-$	3.76	4.12	2.93(g), <sup>20</sup> 3.63(l), <sup>26</sup> 3.10(l) <sup>21</sup>		3.35, <sup>41</sup> 3.63, <sup>40</sup> 2.76, <sup>46</sup> 2.81, <sup>48</sup> 2.92 <sup>49</sup>	
Anthracene (C <sub>14</sub> H <sub>10</sub> )						
$1^3B_{2u}^+$	1.73	1.48	1.82(l), <sup>17,18</sup> 1.87(g) <sup>74</sup>		1.72, <sup>43</sup> 2.0, <sup>53</sup> 1.8, <sup>55</sup> 1.66, <sup>40</sup> 1.81, <sup>54</sup> 1.99, <sup>52</sup> 1.45 <sup>45</sup>	
$1^3B_{1g}^+$	1.22	1.10	1.40(l) <sup>21</sup>		1.18, <sup>40</sup> 1.35 <sup>49</sup> 1.42, <sup>45</sup>	
$1^3A_g^+$	2.31	2.11	2.65(l), <sup>26</sup> 2.40(l) <sup>21</sup>		2.32, <sup>40</sup> 2.62, <sup>49</sup> 3.70 <sup>45</sup>	
$1^3B_{1g}^-$	3.30	3.09	3.24(g), <sup>24</sup> 3.07(g), <sup>23</sup> 2.92(l) <sup>21,26</sup>		3.35, <sup>45</sup> 3.28, <sup>40</sup> 4.65, <sup>42</sup> 2.74 <sup>50</sup>	
$1^3A_g^-$	3.84	3.96	3.77(l) <sup>21</sup>		4.16, <sup>45</sup> 3.32, <sup>40</sup> 4.24, <sup>42</sup> 3.03 <sup>50</sup>	
Tetracene(C <sub>18</sub> H <sub>12</sub> )						
$1^3B_{2u}^+$	1.25	1.11	1.25(s) <sup>75</sup> 1.27(l), <sup>22</sup> 1.30(l) <sup>25</sup>		1.22, <sup>44</sup> 1.39, <sup>53</sup> 1.12, <sup>55</sup> 1.33, <sup>76</sup> 1.10, <sup>40</sup> 1.20, <sup>54</sup> 1.51 <sup>52</sup>	
$1^3B_{1g}^+$	1.09	1.04	1.29(l) <sup>21</sup>		1.24, <sup>45</sup> 0.763, <sup>40</sup> 0.92, <sup>50</sup>	
$1^3A_g^+$	2.55	2.42	2.58(l), <sup>21,31</sup> 2.60(l) <sup>26</sup>		2.65, <sup>40</sup> 2.93 <sup>50</sup>	
$1^3B_{1g}^-$	3.05	2.79	2.92(g), <sup>23</sup> 2.69(l), <sup>26</sup> 2.68(l), <sup>21</sup> 2.55(l) <sup>27</sup>		3.07, <sup>44</sup> 2.97, <sup>45</sup> 3.16, <sup>40</sup> 2.51 <sup>50</sup>	
$1^3A_g^-$	3.82	3.91	3.95(l), <sup>26</sup> 3.66(l), <sup>21</sup> 3.01(l) <sup>27</sup>		3.82, <sup>44</sup> 4.23, <sup>45</sup> 3.39, <sup>40</sup> 3.26 <sup>50</sup>	

overestimates our calculated value. On comparing with the experiments, the best estimate of the excitation energy for the state  $1^3B_{2u}^+$ , from the simulations, is 2.67 eV by Hachmann *et al.*<sup>52</sup>

For the dipole forbidden state  $1^3B_{1g}^+$ , Meyer *et al.*,<sup>21</sup> based upon their solution based

Table IV. Comparison of results of our triplet calculations for pentacene, hexacene, and heptacene ( $n = 5 - 7$ ) performed with the standard (std.) parameters and the screened (scr.) parameters with other experimental and theoretical results for the most important low-lying states. The energies of the  $1^3B_{1g}^-$  and  $1^3A_g^-$  states are given with respect to the  $1^3B_{2u}^+$  state.

State	Excitation energy (eV)				
	Present work		Experimental	Other theoretical	
	std.	scr.			
Pentacene( $C_{22}H_{14}$ )					
$1^3B_{2u}^+$	0.99	0.93	0.95(1), <sup>77</sup> 0.86±0.03(s) <sup>28</sup>	0.53, <sup>45</sup> 0.91, <sup>43</sup> 1.05, <sup>53</sup> 0.99, <sup>33</sup> 0.88, <sup>51</sup> 0.99, <sup>76</sup> 0.79, <sup>40</sup> 0.78, <sup>54</sup> 1.16 <sup>52</sup>	
$1^3B_{1g}^+$	0.96	0.90		0.88, <sup>40</sup> 1.06, <sup>45</sup> 1.24 <sup>51</sup>	
$1^3A_g^+$	2.67	2.44		2.90, <sup>40</sup> 4.15 <sup>45</sup>	
$1^3B_{1g}^-$	2.87	2.54	2.53(1), <sup>26</sup> 2.46(1) <sup>29</sup>	2.76, <sup>45</sup> 2.89 <sup>40</sup>	
$1^3A_g^-$	3.77	3.79	3.16(1) <sup>29</sup>	4.40, <sup>45</sup> 3.43, <sup>40</sup>	
Hexacene( $C_{26}H_{16}$ )					
$1^3B_{2u}^+$	0.87	0.85	0.54±0.05(1) <sup>30</sup>	0.73, <sup>53</sup> 0.46, <sup>54</sup> 0.45, <sup>62</sup> 0.91 <sup>52</sup>	
$1^3B_{1g}^+$	0.80	0.75			
$1^3A_g^+$	2.63	2.25			
$1^3B_{1g}^-$	2.70	2.33	2.25(1) <sup>30</sup>	2.18, <sup>57</sup> 2.42 <sup>30</sup>	
$1^3A_g^-$	3.74	3.65			
Heptacene( $C_{30}H_{18}$ )					
$1^3B_{2u}^+$	0.73	0.69		0.54, <sup>53</sup> 0.24 <sup>54</sup>	
$1^3B_{1g}^+$	0.69	0.61			
$1^3A_g^+$	2.34	1.90			
$1^3B_{1g}^-$	2.58	2.14	2.14(1) <sup>12</sup>		
$1^3A_g^-$	3.72	3.17			

measurement of triplet-triplet absorption spectra of naphthalene, anthracene and tetracene using transient absorption spectroscopy, reported  $E(1^3B_{1g}^+) - E(1^3B_{2u}^+)$  to be in the range 1.30-1.35 eV, a value which is in good agreement with our standard parameter based value of 1.21 eV. Our screened parameter value 1.16 eV underestimates the experimental value

somewhat. Coupled-cluster calculations, CC3 with TZVP basis set, by Thiel et al,<sup>72</sup> predicts 1.36 eV as the value, which matches perfectly with the experiment. Other reported theoretical values for this quantity is 1.14 eV calculated using the CASPT2 approach.<sup>48</sup>

For the state  $1^3A_g^+$ , there are two reported experimental values of  $E(1^3A_g^+) - E(1^3B_{2u}^+)$ , 1.97 eV<sup>21</sup> based upon the solution phase data, and 2.25 eV obtained by Hunziker<sup>20</sup> from the gas phase experiments, using kinetic spectroscopy based on modulated excitation of mercury-photo-sensitized reactions, in the visible absorption regions of the spectrum.

Our screened parameter value of 1.97 eV matches exactly with the solution phase results,<sup>21</sup> while the standard parameter value of 2.06 eV is in between the two experimental values. As far as the theoretical works of other authors are concerned, Rubio et al.<sup>48</sup> obtained 2.18 eV using the CASPT2 approach, while the value 2.41 eV reported by Thiel *et al.*,<sup>72</sup> overestimates our calculated value. On comparing with the experiments, the best estimate of the excitation energy for the state  $1^3A_g^+$ , 1.97 eV is from our screened parameter calculation.

For the long-axis polarized dipole allowed state  $1^3B_{1g}^-$ , the reported experimental values of  $E(1^3B_{1g}^-) - E(1^3B_{2u}^+)$  are in the range 2.98—3.12 eV,<sup>19,21,23,26</sup> while for the short-axis polarized  $1^3A_g^-$  state the corresponding values fall in the range 2.93—3.63 eV.<sup>20,21,26</sup> As far as experimental techniques employed are concerned, Porter and Wright<sup>23</sup> used flash photolysis technique to measure the triplet absorption spectra of naphthalene, anthracene and tetracene in the gas phase, whereas the same for naphthalene, anthracene, tetracene and pentacene, in fluid solutions at normal temperature was measured by Porter and Windsor<sup>26</sup> using again the flash photolysis and transient absorption spectroscopy. Hunziker used the absorption of light emitted by Hg atoms in the triplet state, and the modulation technique, to observe triplet absorption in naphthalene in the gas phase.<sup>19</sup> Our calculated values for  $E(1^3B_{1g}^-) - E(1^3B_{2u}^+)$  3.50 eV (screened parameters) and 3.60 eV (standard parameters) appear to overestimate corresponding experimental values. Reported theoretical values of other authors range from 2.61 eV to 3.52 eV (*cf.* Table III), obtained using a variety of methods.<sup>40,41,46,48,49</sup> For the  $1^3A_g^-$  state, our standard parameter value 3.76 eV for  $E(1^3A_g^-) - E(1^3B_{2u}^+)$  is in excellent agreement with 3.63 eV measured by Porter and Windsor<sup>26</sup> in the solution phase. Other authors have reported theoretical values of this quantity in the range 2.76—3.63 eV.<sup>40,41,46,48,49</sup> As far as agreement with the gas-phase experimental values for the excitation energies of  $1^3B_{1g}^-$  and  $1^3A_g^-$  is concerned, the best theoretical estimates appear to be 2.71 eV and 2.92 eV, respectively, obtained by Hirao and co-workers, using MRMP



method, with cc-pVDZ basis set.<sup>49</sup>

## 2. Anthracene

Like naphthalene, for anthracene also several experimental and theoretical investigations have been performed over the years. In early solution based experiments Lewis and Kasha,<sup>17</sup> as well as McClure<sup>18</sup> reported the value of  $E(1^3B_{2u}^+)$  to be 1.82 eV, while in a more recent gas phase experiment using photodetachment photoelectron spectroscopy of anthracene, Schiedt and Weinkauff<sup>74</sup> measured it to be 1.87 eV. Here again the standard parameter value of 1.78 eV is in significantly better agreement with the experiments as compared to the screened parameter value of 1.48 eV. Similar to the case of naphthalene, even other theoretical calculations also match well with our standard parameter value. Ramasesha *et al.*, based upon PPP-FCI calculations reported  $E(1^3B_{2u}^+)$  as 1.71 eV,<sup>78</sup> Houk *et al.*<sup>54</sup> based upon DFT calculations, and Quarti *et al.*<sup>55</sup> relying on a variety of quantum-chemical calculations reported it to be 1.8 eV, while Hachmann *et al.*<sup>52</sup> and Hajgato *et al.*<sup>53</sup> computed it as 2.0 eV. On comparing with the experiments, the best estimate of the excitation energy for the state  $1^3B_{2u}^+$ , is 1.81 eV, obtained by Houk and co-workers, using B3LYP as exchange-correlation functional with a 6-31G\* basis sets.<sup>54</sup>

For the dipole forbidden state  $1^3B_{1g}^+$ , the reported experimental value of  $E(1^3B_{1g}^+) - E(1^3B_{2u}^+)$  1.40 eV<sup>21</sup> is closer to our standard parameter value 1.22 eV as compared to the screened parameter one. Theoretical works of other authors lie in the range 1.18—1.42 eV.<sup>40,45,49</sup> For the higher dipole forbidden state  $1^3A_g^+$ , two experimental values 2.40 eV<sup>21</sup> and 2.65 eV<sup>26</sup> based upon the liquid phase data have been reported, and both are in better agreement with our standard parameter value 2.31 eV, as compared to the screened one. Theoretical values reported by other authors for  $E(1^3A_g^+) - E(1^3B_{2u}^+)$  are 2.32 eV,<sup>40</sup> 2.62 eV,<sup>49</sup> in good agreement with our standard parameter results. On comparing with the experiments, the best estimates of the excitation energies for the states  $1^3B_{1g}^+$  and  $1^3A_g^+$ , 1.35 eV and 2.62 eV, respectively, were obtained by Hashimoto *et al.*, using MRMP method, cc-pVDZ basis set.<sup>49</sup>

For the dipole allowed state  $1^3B_{1g}^-$ , the value of  $E(1^3B_{1g}^-) - E(1^3B_{2u}^+)$  from solution based experiments was reported to be 2.92 eV,<sup>21,26</sup> while gas phase experiments report two distinct values 3.07 eV,<sup>23</sup> and 3.24 eV.<sup>24</sup> For the gas-phase experiment reporting the larger value,<sup>24</sup> the

technique employed was electron energy loss spectroscopy. Interestingly, both our screened and standard parameter values are in good agreement with the two gas phase results.

For the short-axis polarized dipole allowed state  $1^3A_g^-$ , only available experimental value of  $E(1^3A_g^-) - E(1^3B_{2u}^+)$  is 3.77 eV, measured in the solution phase.<sup>21</sup> Our standard parameter value of 3.84 eV is in excellent agreement with this value, while the screened parameter value 3.96 eV overestimates it a bit. Other theoretical values of this quantity are distributed in the wide range 3.03—4.24 eV.<sup>40,42,45,50</sup> Upon comparing with the experiments, the best estimates of the excitation energies of the dipole-allowed states,  $1^3B_{1g}^-$ , and  $1^3A_g^-$ , are 3.30 eV, and 3.84 eV, respectively, obtained in our standard parameter calculation.

### 3. Tetracene

For tetracene, the value of  $E(1^3B_{2u}^+)$  1.25 eV was obtained by Tomkiewicz *et al.*<sup>75</sup> by measuring the singlet-triplet spectrum in solid phase as observed in the delayed fluorescence from a tetracene crystal at room temperature. Liquid phase experiments of Mc Glynn *et al.*<sup>22</sup> yielded the value 1.27 eV, while Sabbatini *et al.*<sup>25</sup> measured it to be 1.30 eV, from the emission spectra of the triplet states of naphthalene, anthracene and tetracene in acetonitrile solution. These experimental values are in closer agreement with our standard parameter based value of 1.25 eV, as compared to the screened parameter value 1.11 eV. In a recent remarkable theoretical work, Pati and Ramasesha managed to perform PPP-FCI calculations for anthracene,<sup>44</sup> and their  $E(1^3B_{2u}^+)$  value of 1.22 eV is in excellent agreement with our standard parameter result obtained using the QCI approach. Theoretical calculations by other authors predict this energy to be in the range 1.10—1.51 eV.<sup>40,52–55,76</sup> In terms of the level of electron correlations taken into account, Pati and Ramasesha's<sup>44</sup> PPP-FCI calculations are the best, although our PPP-QCI value obtained with standard parameters is in marginally better agreement with the experiments.

For the dipole forbidden state  $1^3B_{1g}^+$ , only one reported experimental value of  $E(1^3B_{1g}^+) - E(1^3B_{2u}^+)$  1.29 eV<sup>21</sup> is based upon liquid phase measurement. Our calculated values are lower than this, with the standard parameter value of 1.09 eV, being somewhat better than the screened parameter value 1.04 eV. Among the theoretical works of other authors, only the value 1.24 eV computed by Lipari and Duke<sup>45</sup> is in better agreement with the experiments as compared to our results, and appears to be the best theoretical estimate. For the other dipole

forbidden state  $1^3A_g^+$ , solution based measurements yield values of  $E(1^3A_g^+) - E(1^3B_{2u}^+)$  as 2.58 eV,<sup>21</sup> and 2.60 eV,<sup>26</sup> while Burdett and Bardeen,<sup>31</sup> using transient absorption and photoluminescence experiments on crystalline tetracene obtained it to be 2.58 eV. Thus, experimental values are close to each other, and also are in close agreement with our standard parameter value 2.55 eV, which also happens to be in best agreement, among all theoretical values, with the experiments. Other reported theoretical values of this quantity overestimate the experiments (*cf.* Table III).

As in the case of anthracene, for the first dipole allowed state  $1^3B_{1g}^-$ , significant variation in the experimental values of  $E(1^3B_{1g}^-) - E(1^3B_{2u}^+)$  is observed. Porter and Wright<sup>23</sup> measured it to be 2.92 eV in gas phase, which is in excellent agreement with our standard parameter value of 3.05 eV. Pavlopoulos<sup>27</sup> reported experimental value of 2.55 eV based upon solution phase measurements of the triplet-triplet absorption spectrum of tetracene using continuous wave (cw) laser excitation, while values obtained in other liquid phase experiments are 2.68 eV,<sup>21</sup> and 2.69 eV.<sup>26</sup> These values, quite expectedly, are in better agreement with our screened parameter value 2.79 eV, as compared to the standard parameter result. As far as theoretical results of other authors are concerned, recent PPP-FCI value 3.07 eV reported by Pati and Ramasesha<sup>44</sup> is in excellent agreement with our standard parameter value, while other reported values in the literature fall in the range 2.51–3.16 eV.<sup>40,45,50</sup>

For the higher dipole allowed state  $1^3A_g^-$ , even though all the experimental measurements of  $E(1^3A_g^-) - E(1^3B_{2u}^+)$  were performed in the liquid phase, yet they exhibit significant variation with reported values 3.01 eV,<sup>27</sup> 3.66 eV,<sup>21</sup> and 3.95 eV.<sup>26</sup> Because of this variation, both our standard and screened parameter values are in good agreement with one experimental value or another (*cf.* Table III). As shown in Table III, theoretical values of this quantity computed by other authors also exhibit wide variation, with our standard parameter results being in perfect agreement with the PPP-FCI values reported by Pati and Ramasesha.<sup>44</sup> On comparing with the liquid phase experiments, the best theoretical estimates of the excitation energies for the states  $1^3B_{1g}^-$  and  $1^3A_g^-$ , 2.79 eV and 3.91 eV, respectively, are from our screened parameter calculations.

#### 4. Pentacene

Pentacene is one of the most widely studied polyacene, and extremely important from the point of view of singlet fission problem, currently being studied vigorously.<sup>4,5</sup> Nijegorodov *et al.*<sup>77</sup> measured the value of  $E(1^3B_{2u}^+)$  to be 0.95 eV in a liquid phase experiment using UV-visible absorption spectroscopy. Burgos *et al.*<sup>28</sup>, on the other hand, obtained the value 0.86 eV by performing fluorescence measurements of pentacene in a solid phase experiment. Both our standard parameter value 0.99 eV, and screened parameter value of 0.93 eV, are in good agreement with the liquid phase measurement. Furthermore, quite expectedly, the screened parameter value is closer to the solid state measurement as compared to the standard parameter result. A large number of theoretical calculations have been performed for this quantity for pentacene, and they range from a low value of 0.53 eV obtained in a CNDO/S2-CI calculation,<sup>45</sup> to a high value of 1.16 eV obtained from a DMRG calculation.<sup>52</sup> However, several other calculations predict values in good agreement with our work, and with the experiments.<sup>33,43,51,76</sup> On comparing with the liquid phase experiments, besides our own screened parameter results, the best theoretical values of the excitation energy of the state  $1^3B_{2u}^+$  were predicted by PPP-DMRG calculations of Raghu *et al.*,<sup>43</sup> and time-dependent density-functional-theory (TDDFT) calculations of Anger *et al.*<sup>33</sup> On the other hand TDDFT results of Zimmerman *et al.*,<sup>51</sup> agree well with solid phase experimental value.

To the best of our knowledge, no experimental measurements of the dipole forbidden states  $1^3B_{1g}^+$  and  $1^3A_g^+$  exist for pentacene, therefore, we will restrict the comparison of our results on these states to the theoretical works of other authors. Pariser<sup>40</sup> computed the value of  $E(1^3B_{1g}^+) - E(1^3B_{2u}^+)$  to be 0.88 eV, while Lipari and Duke predicted it to be 1.06 eV, both of which are in reasonable agreement with our computed values. The TDDFT value of 1.24 eV calculated by Zimmerman *et al.*<sup>51</sup> for the quantity is substantially larger than our prediction. For the  $1^3A_g^+$  state our calculated values of  $E(1^3A_g^+) - E(1^3B_{2u}^+)$  2.44 eV (screened), and 2.67 eV (standard), are lower compared to the PPP-SCI value 2.90 eV reported by Pariser,<sup>40</sup> but significantly smaller compared to 4.15 eV calculated by Lipari and Duke.<sup>45</sup> Given the uncertainty in the theoretical excitation energies of these dipole forbidden states, it will be good if measurements are performed on these states of pentacene in future.

For the long-axis polarized dipole-allowed state  $1^3B_{1g}^-$ , two liquid phase experimental val-

ues of  $E(1^3B_{1g}^-) - E(1^3B_{2u}^+)$  2.46 eV,<sup>29</sup> obtained using flash photolysis, absorption spectrum of triplet pentacene in benzene and cyclohexane at 50°C, and 2.53 eV reported by Porter and Windsor,<sup>26</sup> are in excellent agreement with our calculated screened parameter value 2.54 eV, while the standard parameter approach predicts a larger value. Theoretical calculations by other authors<sup>40,45</sup> (*cf.* Table IV) predict values larger than the experimental one, and are in better agreement with our standard parameter calculation. Therefore, as far as the agreement with the experimental results is concerned, the best estimate of the excitation energy of the state  $1^3B_{1g}^-$ , is 2.54 eV predicted by our screened parameter calculation.

For the other dipole allowed state  $1^3A_g^-$ , we have an anomaly vis-a-vis experiments in that the only available experimental value of  $E(1^3A_g^-) - E(1^3B_{2u}^+)$  3.16 eV,<sup>29</sup> is substantial smaller than all the calculated theoretical values, including our own. Therefore, it will be quite useful if an experiment could be repeated on pentacene to ascertain the excitation energy of this state.

### 5. Hexacene and Heptacene

Very few experiments have been performed on the triplet states of higher acenes such as hexacene and heptacene, perhaps because of difficulties associated with their synthesis. As a result, the number of theoretical calculations on these compounds are relatively small. For hexacene, based on a liquid phase experiment, Angliker *et al.*<sup>30</sup>, using the absorption spectra of triplet hexacene, by flash photolysis, estimated the value of  $E(1^3B_{2u}^+)$  to be 0.54 eV, which is substantially smaller than our computed values 0.85 eV (screened) and 0.87 eV (standard). This reported experimental value is also not in agreement with the theoretical works of other authors whose values are either significantly smaller than it, or larger than it (*cf.* Table IV). In the same experiment, Angliker *et al.*<sup>30</sup> measured  $E(1^3B_{1g}^-) - E(1^3B_{2u}^+)$  to be 2.25 eV which is actually in very good agreement with our screened parameter value 2.33 eV. Angliker *et al.*<sup>30</sup> also calculated the value of this excitation energy using the PPP-SCI approach using a different set of Coulomb parameters, and obtained the value 2.42 eV, which is in good agreement with our screened parameter result. DFT based calculations of Nguyen *et al.*<sup>57</sup> predict the value of this energy as 2.18 eV, which is close to the experimental value, but somewhat smaller than our screened parameter result. Thus, on comparing with the experiments, the best estimate of the excitation energy for the state  $1^3B_{2u}^+$ , 0.45-0.46 eV by

Houk and co-workers,<sup>54,62</sup> using B3LYP method, 6-31G\* basis set, and for the state  $1^3B_{1g}^-$ , 2.33 eV obtained in our screened parameter calculation.

For heptacene, to the best of our knowledge, no experimental measurements of  $E(1^3B_{2u}^+)$  exist. Theoretical calculations by Hajgato *et al.*<sup>53</sup> predict it to be 0.54 eV, while the DFT based work of Houk *et al.*<sup>54</sup> estimates a rather small value of 0.24 eV. From Table IV it is obvious that our calculated values are larger than these results, with a somewhat better agreement between the work of Hajgato *et al.*<sup>53</sup> and our screened parameter estimate. However, liquid phase experiment on the dipole allowed  $1^3B_{1g}^-$  state of heptacene performed by Mondal *et al.*<sup>12</sup> using nanosecond laser flash photolysis and femtosecond pump-probe UV-vis spectrometry, measured  $E(1^3B_{1g}^-) - E(1^3B_{2u}^+)$  to be 2.14 eV, which is in exact agreement with our screened parameter result, thus giving us confidence about the quality of our calculations even for a relatively longer oligoacene such as heptacene.

## B. Triplet Absorption Spectrum

First singlet excited state  $S_1$  ( $1^1B_{2u}^+$ , in the present case) of conjugated molecules frequently decays to the first triplet excited state  $T_1$  ( $1^3B_{2u}^+$ , in the present case) located below  $S_1$ , through non-radiative inter-system crossing (ISC), as shown in Fig. 2. In case of single crystals or thin films, this transition is believed to occur via singlet fission,<sup>32</sup> whose mechanism is also an area of intense research.<sup>4,5</sup> Once the triplet state is attained, usual optical absorption experiments can be conducted to probe higher triplet states. In case of oligoacenes, according to the electric-dipole selection rules of the  $D_{2h}$  point group, the transitions from the  $1^3B_{2u}^+$  to  $3^3B_{1g}^-$  type of states is caused by the long-axis ( $x$ -axis) polarized photons, whereas the transitions to the  $3^3A_g^-$  type states by the short-axis ( $y$ -axis) polarized ones (*cf.* Fig. 2). In figs. 4—9, we present the triplet absorption spectra of naphthalene to heptacene, while the wave functions of the excited states contributing to peaks in the spectra, along with corresponding transition dipole moments, are presented in Tables V—XVI of Appendix B. Next, we summarize the salient features of the triplet absorption spectra, and briefly discuss the many-particle wave functions of the excited states contributing to it.

### 1. Dipole forbidden spectrum

As mentioned earlier,  $x$ -polarized  $1^3B_{1g}^+$  state, and  $y$ -polarized  $1^3A_g^+$  state do not contribute to the computed spectra because they are dipole forbidden due to the particle-hole symmetry. Nevertheless, in experimental spectra they contribute faint peaks, therefore, we are presenting a discussion of their many-particle wave functions. We note that the wave functions of both these states are dominated by singly excited configurations. On adopting the notation that  $H$  denotes the highest occupied molecular orbital (HOMO), and  $L$  denotes the lowest unoccupied molecular orbital (LUMO), we find that the wave function of the  $1^3B_{1g}^+$  state has dominant contributions from  $|H \rightarrow L + 2\rangle$  and *c.c.* (*c.c.* denotes the electron-hole conjugate configuration), for naphthalene and anthracene, and from single excitations  $|H \rightarrow L + 1\rangle$  and *c.c.*, for tetracene up to heptacene, irrespective of the choice of Coulomb parameters. On the other hand,  $1^3A_g^+$  state has dominant contributions from excitations  $|H \rightarrow L + 3\rangle + c.c.$  for the case of naphthalene and anthracene, from the single excitations  $|H \rightarrow L + 4\rangle + c.c.$  for tetracene up to hexacene, but from double excitation  $|H \rightarrow L; H - 1 \rightarrow L + 1\rangle$ , for heptacene, irrespective of the choice of Coulomb parameters. Dominant contribution from double excitation also points to the increased electron-correlation effects contributing to this state.

### 2. Dipole allowed spectrum

In a recent work, we calculated the triplet absorption spectra of longer oligoacenes namely octacene, nonacene and decacene, with an aim to understand their experimentally measured optical absorption.<sup>59</sup> In this section we analyze the similarities and differences between the triplet absorption spectra of shorter acenes (naphthalene to heptacene), when compared to those of the longer ones (octacene, nonacene and decacene).

As far as the similarities between the short and the long acenes are concerned, irrespective of the length of acene, triplet spectrum of a given acene computed using the screened parameters exhibits a red shift as compared to the one calculated using the standard parameters. Moreover, the  $x$ -polarized (long-axis polarized) spectra, corresponding to the absorption into the  $^3B_{1g}^-$  type of states is quite intense, while the  $y$ -polarized absorption into the  $^3A_g^-$  type states is found to be rather weak. In addition, it is evident from the triplet absorption

spectra of each oligoacene calculated using either of the Coulomb parameters, that there are two prominent intense  $x$ -polarized peaks which are well separated in energy ( $>1.5$  eV). Furthermore, the many-particle wave function of the Peak I, corresponding to the state,  $1^3B_{1g}^-$  is dominated by singly-excited configurations  $|H \rightarrow L + 1\rangle + c.c.$ , for the oligomers from tetracene up to decacene, irrespective of the choice of Coulomb parameters, except for the case of naphthalene and anthracene, where singly-excited configurations  $|H \rightarrow L + 2\rangle + c.c.$  dominate the many-particle wave function of the same peak. Other peaks in the spectra correspond to either  $x$  or  $y$  polarized transitions to the higher excited states of the system, information about which is presented in the tables in Appendix B.

Next, we elucidate some of the important differences we have observed between the computed triplet spectra of short and long acenes. In our work on the longer acenes we found that, out of the two intense  $x$ -polarized peaks, the first one (peak I) is the most intense one in the screened parameter calculations, while the second one (peak IV or V) has maximum intensity in the standard parameter results.<sup>59</sup> However, in the present work on shorter acenes, the trend is somewhat different in that, irrespective of the choice of the Coulomb parameters employed, of the two strong peaks, first peak (I) is always the second most intense one, while, in all the cases, the most intense peak is the second one (III, IV or V, depending on the size of the oligomer). As far as the excited state wave functions are concerned, for a longer acene of length  $n$  ( $=8-10$ ), in the screened parameter calculations, the wave function of the state corresponding to the second intense peak (IV or V) consists of  $|H \rightarrow L; H - (n/2 - 1) \rightarrow L\rangle + c.c.$  for  $n \equiv \text{even}$ , and  $|H \rightarrow L; H - (n - 1)/2 \rightarrow L\rangle + c.c.$ , for  $n \equiv \text{odd}$ .<sup>59</sup> With the standard parameters, for the same oligomer the main configurations contributing to the peak were  $|H \rightarrow L; H - n/2 \rightarrow L\rangle + c.c.$  for  $n \equiv \text{even}$ , and  $|H \rightarrow L; H - (n - 1)/2 \rightarrow L\rangle + c.c.$ , for  $n \equiv \text{odd}$ .<sup>59</sup> Whereas, in the current work on shorter acenes ( $n = 2-7$ ), irrespective of the choice of Coulomb parameters, the wave function corresponding to the second intense peak (III, IV or V) mainly consists of double excitations  $|H \rightarrow L; H - n/2 \rightarrow L\rangle + c.c.$  for  $n \equiv \text{even}$ , and  $|H \rightarrow L; H - (n - 1)/2 \rightarrow L\rangle + c.c.$ , for  $n \equiv \text{odd}$ .



Figure 4. Triplet optical absorption spectra of naphthalene from the  $1^3B_{2u}^+$  state computed using the standard parameters (panel (a)), and the screened parameters (panel (b)), and a uniform line width of 0.1 eV. The polarization directions ( $x$  or  $y$ ) are indicated by the subscripts attached to the peak labels.

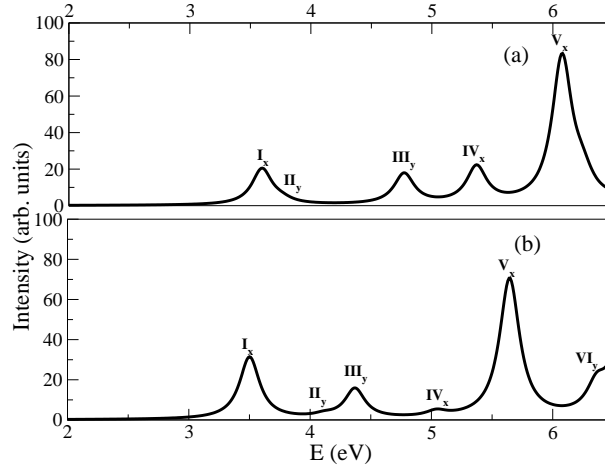


Figure 5. Triplet optical absorption spectra of anthracene from the  $1^3B_{2u}^+$  state computed using the standard parameters (panel (a)), and the screened parameters (panel (b)). The rest of the information is same as in the caption of Fig. 4.

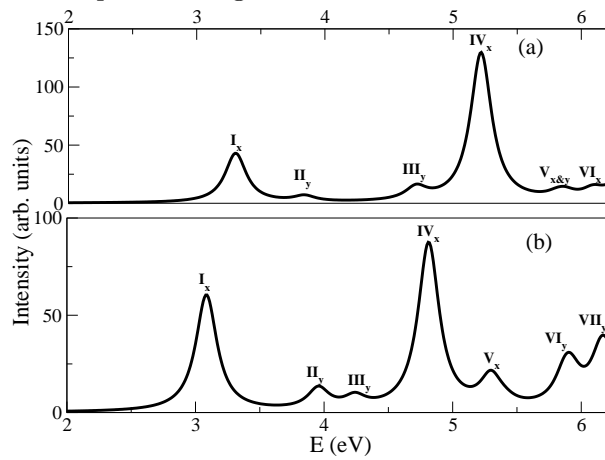


Figure 6. Triplet optical absorption spectra of tetracene from the  $1^3B_{2u}^+$  state computed using the standard parameters (panel (a)), and the screened parameters (panel (b)). The rest of the information is same as in the caption of Fig. 4.

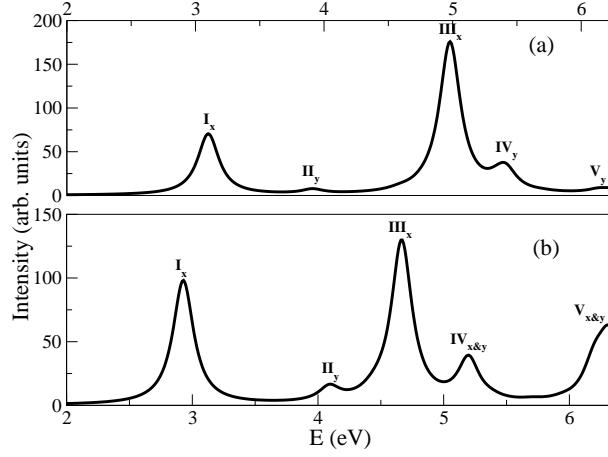


Figure 7. Triplet optical absorption spectra of pentacene from the  $1^3B_{2u}^+$  state computed using the standard parameters (panel (a)), and the screened parameters (panel (b)). The rest of the information is same as in the caption of Fig. 4.

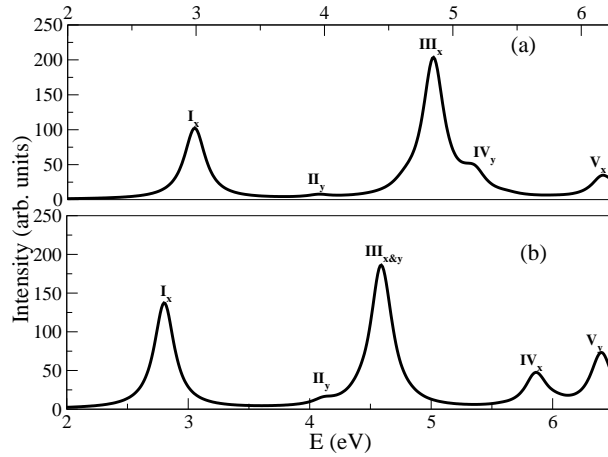


Figure 8. Triplet optical absorption spectra of hexacene from the  $1^3B_{2u}^+$  state computed using the standard parameters (panel (a)), and the screened parameters (panel (b)). The rest of the information is same as in the caption of Fig. 4.

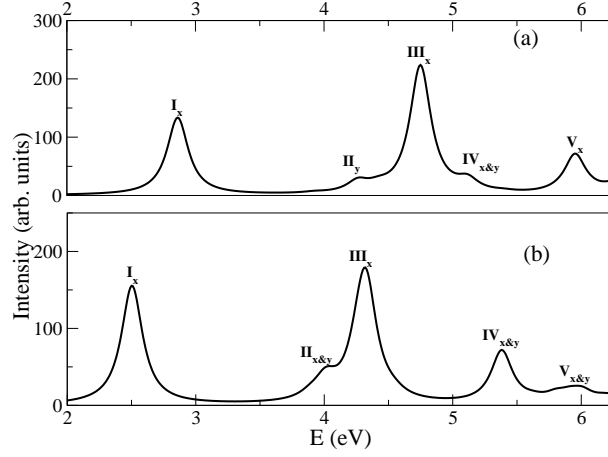
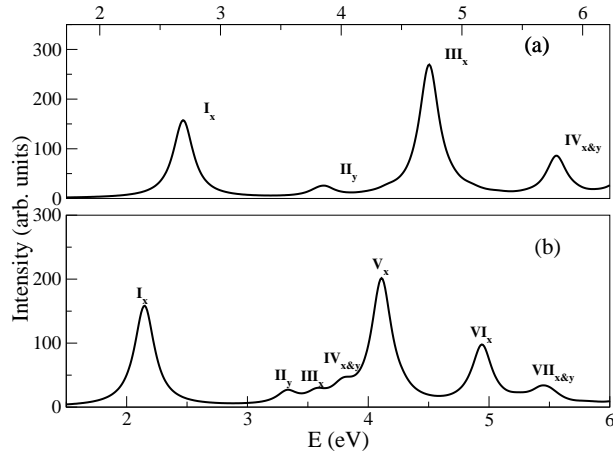


Figure 9. Triplet optical absorption spectra of heptacene from the  $1^3B_{2u}^+$  state computed using the standard parameters (panel (a)), and the screened parameters (panel (b)). The rest of the information is same as



### C. Comparison with poly-(para)phenylene vinylene chains

Several years back, one of us performed a systematic study of triplet states and triplet optical absorption in oligomers of poly-(para)phenylene vinylene (PPV).<sup>6</sup> Next we compare

our earlier results on PPV with the present ones on oligoacenes. In finite PPV chains excitation energy of  $T_1$  ( $1^3B_u^+$  state) exhibited almost complete saturation starting from the two-unit oligomer, implying that  $T_1$  is highly localized in PPV, and essentially has a Frenkel exciton character.<sup>6</sup> However, it is obvious from Tables III and IV, and also from our earlier work on longer acenes,<sup>59</sup> that the excitation energy of  $T_1$  ( $1^3B_{2u}^+$ ) for oligoacenes exhibits no signs of saturation with increasing length, implying that, if  $T_1$  for polyacene is an exciton in the thermodynamic limit, it is a highly delocalized one, similar to a Wannier exciton.

When we compare the triplet absorption spectra of PPV chains<sup>6</sup> with those of oligoacenes, following differences emerge: (a) the first peak in the absorption spectrum of PPV chains is always the most intense one, while in case of oligoacenes the first peak is always the second most intense peak, and (b) successive peaks in case of PPV chains exhibit a pattern of alternating high and low intensities, while no such pattern is visible in case of oligoacenes.

In an earlier work, Shimoi and Mazumdar<sup>79</sup> had argued that the  $m^3A_g$  state of conjugated polymers, which is the first excited state with a strong dipole coupling to  $T_1$ , is also an exciton, and, therefore, the quantity  $E(m^3A_g) - E(1^1B_u)$  can serve as a lower-limit estimate of the binding energy of the optical exciton ( $1^1B_u$ ). For the case of oligoacenes the first optical state is  $1^1B_{2u}^+$ , while  $m^3A_g$  is the  $1^3B_{1g}^-$  state. Therefore, using the values of  $E(1^3B_{1g}^-)$  computed in this work, and  $E(1^1B_{2u})$  calculated in our earlier work,<sup>16</sup> for heptacene we obtain the values of  $E(m^3A_g) - E(1^1B_u)$  to be 0.68 eV (standard) and 0.59 eV (screened). Our screened parameter value of 0.59 eV obtained for polyacenes is lower than 0.68 eV which we estimated for PPV using the same Coulomb parameters in the PPP model.<sup>6</sup> Furthermore, if we examine the behavior of  $E(m^3A_g) - E(1^1B_u)$  as a function of the length of oligoacene, with both sets of Coulomb parameters a decreasing trend is observed. Therefore, it will be of considerable interest to know whether, in the thermodynamic limit, exciton binding energy defined in this manner saturates to a finite value, or simply vanishes.

#### IV. CONCLUSION

In this work we presented large-scale electron-correlated calculations of the triplet states, as well as triplet-triplet absorption spectra, of oligoacenes ranging from naphthalene to heptacene. Generally very good agreement was observed between our calculations, and available experimental results. For the case of hexacene and heptacene, not much experimental data

is available, therefore, our results on those oligomers could be tested in future experiments. As far as triplet absorption spectrum is concerned, our most important prediction is the presence of two long-axis polarized well-separated peaks, which we hope will be tested in future experiments on oriented samples of oligoacenes. We have also presented a detailed analysis of the wave functions of the important triplet excited states.

When compared to  $T_1$  in PPV, our calculations find that the  $T_1$  in oligoacenes is significantly delocalized, and has a Wannier exciton like character. Furthermore, we have observed that the triplet absorption spectra of polyacenes are qualitatively different as compared to those of the PPV chains. We have also presented numerical estimates of the optical exciton binding energy in oligoacenes, and found it to be less than that in PPV chains. However, these estimates can be significantly improved by performing calculations on longer oligoacenes. Moreover, it will also be of interest to probe the nonlinear optical properties of polyacenes, a topic which we intend to pursue in future works in our group.

## ACKNOWLEDGMENTS

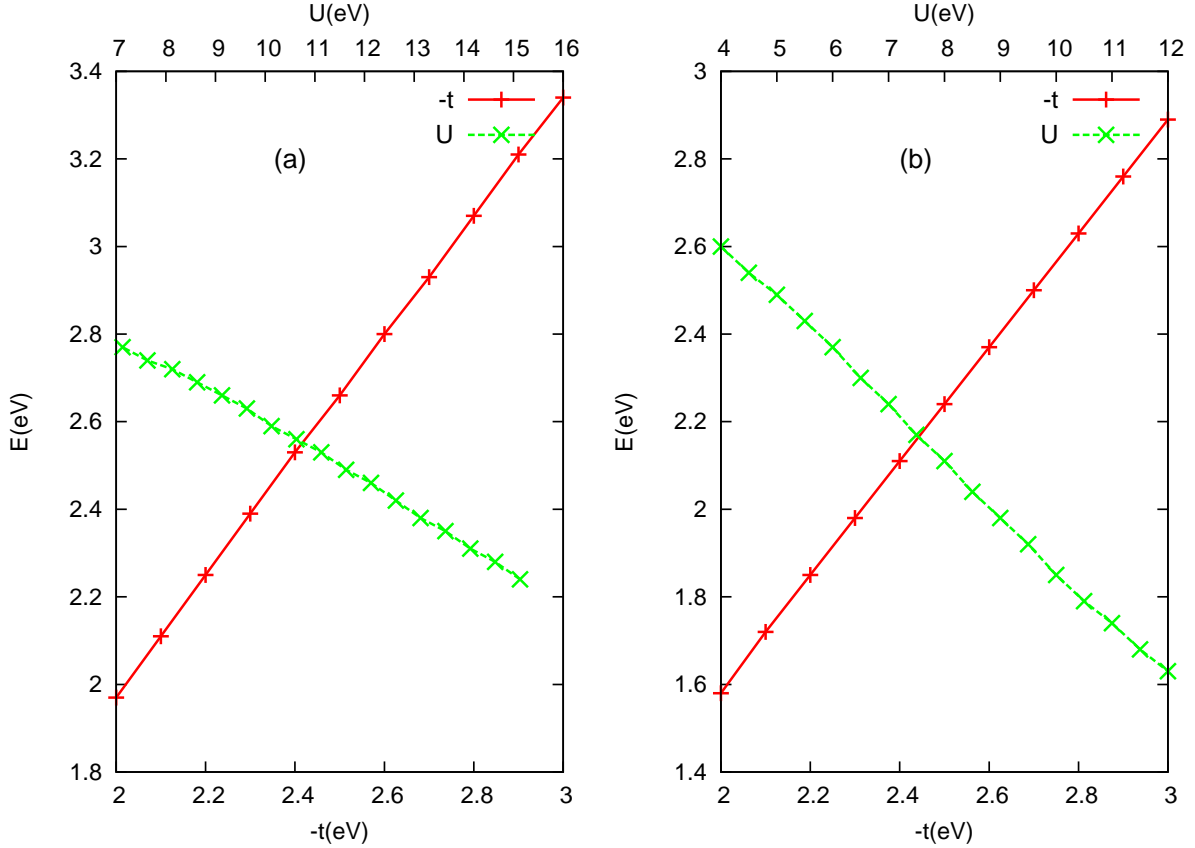
One of us (H.C.) thanks Council of Scientific and Industrial Research (CSIR), India for providing a Senior Research Fellowship (SRF). We thankfully acknowledge the computational resources (PARAM-YUVA) provided for this work by Center for Development of Advanced Computing (C-DAC), Pune.

## Appendix A: Convergence of Lowest Triplet Excitation Energies

### 1. Influence of PPP model parameters on excitation energies

In Fig. 10 we present the plots of the excitation energy of the lowest triplet state,  $1^3B_{2u}^+$ , of naphthalene as a function of the two PPP model parameters: (a) nearest-neighbor hopping matrix element  $t$ , and (b) on-site repulsion energy,  $U$ . The calculations for the purpose were performed using the FCI approach, and both the standard and the screened parameterization schemes described in Sec. II were adopted. In order to examine the influence of variation of  $t$  on the excitation energy, the values of  $U$  was held fixed at 11.13 eV / 8.0 eV for standard/screened parameter calculations, while  $t$  was varied in the range depicted in the plot. Similarly, the influence of variation in  $U$  was examined by holding the hopping fixed at  $t = -2.4$  eV, and varying  $U$  as per standard/screened parameterization schemes, in the range specified in the figure. An inspection of Fig. 10 reveals the following trends both for the standard and the screened parameter based calculations: (a) For the fixed value of  $U$ , with the increasing magnitude of  $t$ , the value of the excitation energy increases, and (b) for the fixed value of  $t$ , with the increasing value of  $U$ , the value of the excitation energy decreases. Furthermore, in ranges of parameters explored in these calculations, variation of the excitation energy is almost linear with respect to both  $t$  and  $U$ . Thus, the behavior the excitation energy of  $1^3B_{2u}^+$  is qualitatively similar with respect to the model parameters, irrespective of the parameterization scheme (standard or screened) employed in the calculations.

Figure 10. Variation of the excitation energy of the lowest triplet state,  $1^3B_{2u}^+$ , of naphthalene as a function of the PPP model parameters  $t$  (nearest-neighbor hopping), and  $U$  (on-site repulsion energy). Calculations were performed using the FCI approach using: (a) standard and, (b) screened-type parameterization.



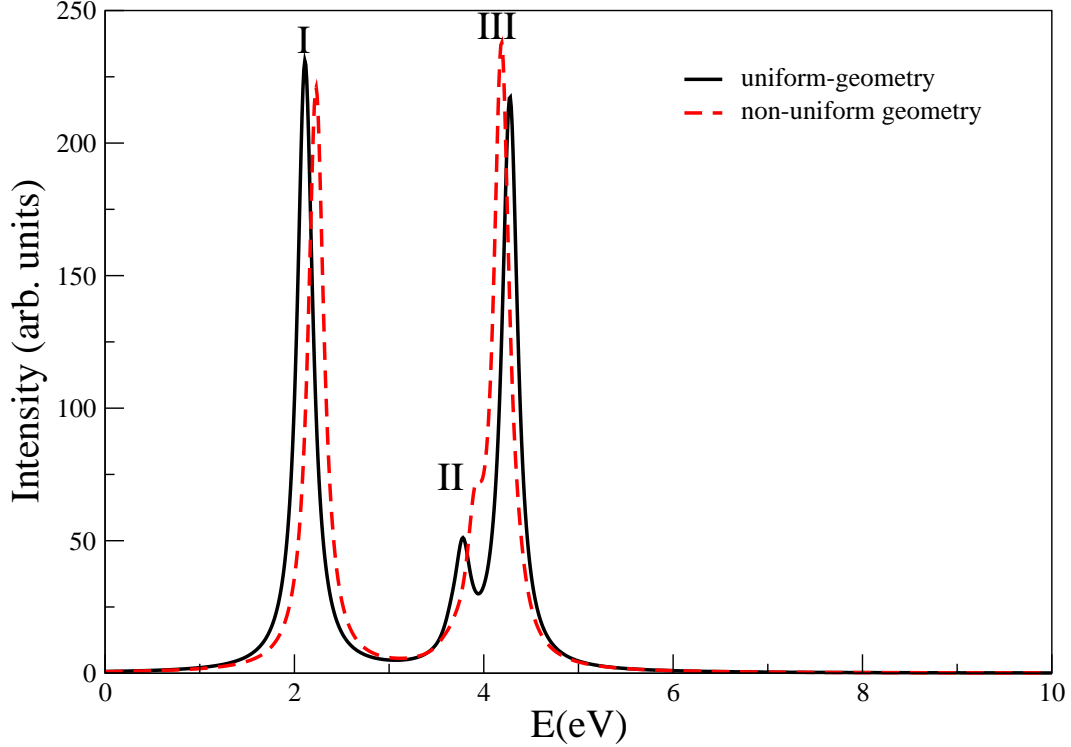
## 2. Influence of geometry on the triplet optical absorption

In this work, consistent with our earlier works,<sup>16,59,80</sup> as also the works of Ramasesha and coworkers,<sup>43,81</sup> we have used the symmetric ground state geometry for all the oligoacenes, with all C-C bonds equal to 1.4 Å, and all bond angles taken to be 120°. In order to investigate the influence of geometry on the triplet optical absorption spectra, we performed calculations on hexacene using a highly non-uniform geometry of  $1^3B_{2u}^+$  state optimized by Houk *et al.*,<sup>54</sup> using B3LYP/6-31G\* calculations. The non-uniformity of this geometry is

obvious from the fact that the smallest C-C bond length in this structure is  $\approx 1.38$  Å, while the largest one is close to 1.47 Å. Similarly, the bond angles in this structure range from  $118.57^\circ$  to  $122.68^\circ$ . For this nonuniform geometry, the hopping matrix elements between nearest-neighbor sites  $i$  and  $j$ , needed for the PPP calculations, were generated using the exponential formula  $t_{ij} = t_0 e^{(r_0 - r_{ij})/\delta}$ , where  $r_{ij}$  is the bond distance (in Å) between the sites,  $t_0 = -2.4$  eV,  $r_0 = 1.4$  Å, and the decay constant  $\delta = 0.73$  Å. The value of  $\delta$  was chosen so that the formula closely reproduces the hopping matrix elements for a bond-alternating polyene with short/long bond lengths 1.35/1.45 Å. The results of SCI level calculations of the triplet optical absorption spectrum of hexacene, both for the uniform (symmetric) and this nonuniform geometry of Houk *et al.*<sup>54</sup> computed using the screened parameters of the PPP model, are presented in Fig. 11. From the figure it is obvious that there are insignificant quantitative differences between the two results, as far as peak locations are concerned. For example, peaks I and II of the nonuniform geometry are blue shifted by about 0.1 eV, while peak III is red shifted by approximately the same amount, as compared to the corresponding peaks obtained using the uniform geometry. Therefore, we conclude that the variations in the geometry of the  $1^3B_{2u}^+$  state of the magnitude considered here, lead to small quantitative, and insignificant qualitative, changes in the triplet optical absorption spectra of oligoacenes.



Fig  
geol

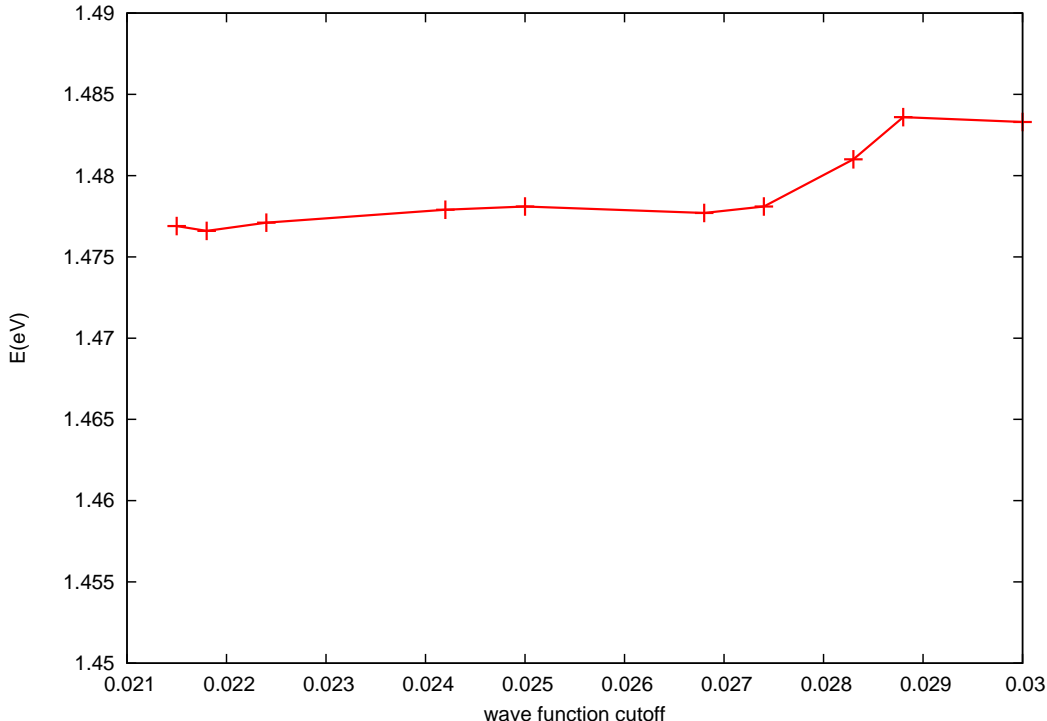


### 3. Convergence of the MRSDCI excitation energies

In this section we demonstrate the convergence of the excitation energy of the  $1^3B_{2u}^+$  state defined as  $E(1^3B_{2u}^+) - E(1^1A_g^-)$ , where  $E(1^3B_{2u}^+)$ , and  $E(1^1A_g^-)$ , respectively, are the total energies of the  $1^3B_{2u}^+$  state and the ground state, computed at a similar level of electron-correlation treatment, employing the MRSDCI approach. The level of correlation treatment in an MRSDCI calculation can be defined either in terms of the number of reference configuration one uses in the calculation, or in terms of the magnitude of the smallest coefficient (henceforth called wave function cutoff) of the configurations included in the reference list. It is obvious that smaller the wave function cutoff, larger the number of configurations in the reference list, and hence larger the total number of configurations in the MRSDCI expansion. Naturally, for accurate results, one must use the same cutoff for both the  $1^3B_{2u}^+$  state as well as  $1^1A_g^-$  ground state. In Fig. 12 we present the results of the MRSDCI calculations of the

excitation energy of the  $1^3B_{2u}^+$  state of anthracene performed using the screened parameters in the PPP model, and the figure depicts the behavior of the excitation energy as a function of the wave function cutoff. We have chosen anthracene, because for this molecule, as reported in Sec. III, FCI results are available, which can be used to benchmark the accuracy of the MRSDCI calculations. From the figure it is obvious that with decreasing value of the wave function cutoff (*i.e.* increasing accuracy of the MRSDCI calculation), the excitation energy converges to a value which is very close to the value 1.48 eV obtained in the FCI calculations, as reported in Table III.

Figure 12. Convergence of the excitation energy of the lowest triplet state  $1^3B_{2u}^+$  of anthracene with respect to the MRSDCI wave function cutoff (see text for an explanation). All calculations were performed using the screened parameters in the PPP model, and the FCI value of the excitation energy is 1.480 eV (*cf.* Table III).



## Appendix B: Calculated Energies, Wave Functions, and Transition Dipole Moments of the Excited States Contributing to the Triplet Absorption Spectra

In this section, we present Tables V—XVI which contain the excitation energies, transition dipole moments, and wave functions of the triplet excited states, which contribute to the calculated triplet absorption spectra of oligoacenes ranging from naphthalene to heptacene, presented in Figs. 4—9 of the main text.

Table V. Properties of the excited states leading to various peaks in the triplet absorption spectrum of naphthalene computed using the FCI method, and the standard parameters in the PPP model Hamiltonian. The table contains excitation energies (with respect to the  $1^1A_g^-$ , ground state), many-particle wave functions, and the transition dipole matrix elements of various states, connecting them to the lowest triplet state  $1^3B_{2u}^+$ . Below, ‘+c.c.’ indicates that the coefficient of the electron-hole conjugate of a given configuration has the same sign, while ‘-c.c.’ implies that they have opposite signs. DF denotes that the concerned excited state is dipole forbidden.

Peak	State	E (eV)	Transition Dipole ( $\text{\AA}$ )	dominant contributing configurations
DF	$1^3B_{1g}^+$	3.74	0.0	$ H \rightarrow L + 2\rangle - c.c.(0.6421)$ $ H - 1 \rightarrow L + 3\rangle + c.c.(0.1200)$
DF	$1^3A_g^+$	4.59	0.0	$ H \rightarrow L + 3\rangle + c.c.(0.5355)$ $ H - 1 \rightarrow L + 2\rangle - c.c.(0.3475)$
I	$1^3B_{1g}^-$	6.13	0.739	$ H \rightarrow L + 2\rangle + c.c.(0.6225)$ $ H \rightarrow L; H \rightarrow L + 1\rangle - c.c.(0.2044)$
II	$1^3A_g^-$	6.29	0.225	$ H - 1 \rightarrow L + 2\rangle + c.c.(0.5890)$ $ H \rightarrow L + 3\rangle - c.c.(0.2993)$
III	$2^3A_g^-$	7.3	0.590	$ H \rightarrow L + 3\rangle - c.c.(0.5469)$ $ H - 1 \rightarrow L + 2\rangle + c.c.(0.2679)$
IV	$2^3B_{1g}^-$	7.9	0.608	$ H - 1 \rightarrow L + 3\rangle - c.c.(0.5168)$ $ H \rightarrow L; H \rightarrow L + 1\rangle - c.c.(0.2928)$
V	$3^3B_{1g}^-$	8.61	1.142	$ H \rightarrow L; H \rightarrow L + 1\rangle - c.c.(0.4939)$ $ H - 1 \rightarrow L + 3\rangle - c.c.(0.2839)$

Table VI. Properties of the excited states leading to various peaks in the triplet absorption spectrum of naphthalene computed using the FCI method, and the screened parameters in the PPP model Hamiltonian. The rest of the information is same as in the caption of Table V.

Peak	State	E (eV)	Transition Dipole ( $\text{\AA}$ )	dominant contributing configurations
DF	$1^3B_{1g}^+$	3.27	0.0	$ H \rightarrow L + 2\rangle + c.c.(0.6148)$ $ H - 1 \rightarrow L + 3\rangle - c.c.(0.1463)$
DF	$1^3A_g^+$	4.08	0.0	$ H \rightarrow L + 3\rangle + c.c.(0.5349)$ $ H - 1 \rightarrow L + 2\rangle - c.c.(0.2822)$
I	$1^3B_{1g}^-$	5.61	0.940	$ H \rightarrow L + 2\rangle - c.c.(0.6447)$ $ H \rightarrow L + 2; H - 3 \rightarrow L\rangle c.c.(0.1033)$
II	$1^3A_g^-$	6.23	0.182	$ H - 1 \rightarrow L + 2\rangle + c.c.(0.5731)$ $ H \rightarrow L + 3\rangle - c.c.(0.3015)$
III	$2^3A_g^-$	6.48	0.579	$ H \rightarrow L + 3\rangle - c.c.(0.5535)$ $ H - 1 \rightarrow L + 2\rangle + c.c.(0.2966)$
IV	$2^3B_{1g}^-$	7.16	0.234	$ H - 1 \rightarrow L + 3\rangle + c.c.(0.5873)$ $ H \rightarrow L; H \rightarrow L + 1\rangle + c.c.(0.2220)$
V	$3^3B_{1g}^-$	7.75	1.109	$ H \rightarrow L; H \rightarrow L + 1\rangle + c.c.(0.5609)$ $ H - 1 \rightarrow L + 3\rangle + c.c.(0.1903)$
VI	$3^3A_g^-$	8.47	0.466	$ H \rightarrow L; H - 1 \rightarrow L + 1\rangle (0.8268)$ $ H \rightarrow L + 3; H - 3 \rightarrow L\rangle (0.2105)$

Table VII. Properties of the excited states leading to various peaks in the triplet absorption spectrum of anthracene computed using the FCI method, and the standard parameters in the PPP model Hamiltonian. The rest of the information is same as in the caption of Table V.

Peak	State	E (eV)	Transition Dipole ( $\text{\AA}$ )	Dominant Contributing Configurations
DF	$1^3B_{1g}^+$	2.95	0.0	$ H \rightarrow L + 2\rangle + c.c.(0.5992)$ $ H - 2 \rightarrow L + 4\rangle + c.c.(0.1889)$
DF	$1^3A_g^+$	4.04	0.0	$ H \rightarrow L + 3\rangle - c.c.(0.5106)$ $ H - 1 \rightarrow L + 2\rangle - c.c.(0.3024)$
I	$1^3B_{1g}^-$	5.03	1.132	$ H \rightarrow L + 2\rangle - c.c.(0.5986)$ $ H \rightarrow L; H \rightarrow L + 1\rangle + c.c.(0.1844)$
II	$1^3A_g^-$	5.57	0.356	$ H - 1 \rightarrow L + 2\rangle + c.c.(0.4912)$ $ H \rightarrow L + 3\rangle + c.c.(0.3989)$
III	$2^3A_g^-$	6.45	0.482	$ H \rightarrow L + 3\rangle + c.c.(0.4523)$ $ H - 1 \rightarrow L + 2\rangle + c.c.(0.3453)$
IV	$2^3B_{1g}^-$	6.95	1.568	$ H \rightarrow L; H \rightarrow L + 1\rangle + c.c.(0.5360)$ $ H - 1 \rightarrow L + 3\rangle - c.c.(0.1850)$
V	$3^3B_{1g}^-$	7.58	0.309	$ H - 1 \rightarrow L + 3\rangle - c.c.(0.3752)$ $ H - 2 \rightarrow L + 4\rangle - c.c.(0.3364)$
	$4^3A_g^-$	7.54	0.236	$ H \rightarrow L; H - 2 \rightarrow L + 2\rangle (0.5992)$ $ H \rightarrow L; H - 1 \rightarrow L + 1\rangle (0.5288)$
VI	$4^3B_{1g}^-$	7.83	0.356	$ H - 2 \rightarrow L + 4\rangle - c.c.(0.4031)$ $ H - 1 \rightarrow L + 3\rangle - c.c.(0.3235)$

Table VIII. Properties of the excited states leading to various peaks in the triplet absorption spectrum of anthracene computed using the FCI method, and the screened parameters in the PPP model Hamiltonian. The rest of the information is same as in the caption of Table V.

Peak	State	E (eV)	Transition Dipole ( $\text{\AA}$ )	Dominant Contributing Configurations
DF	$1^3B_{1g}^+$	2.58	0.0	$ H \rightarrow L + 2\rangle - c.c.(0.5735)$ $ H - 2 \rightarrow L + 4\rangle + c.c.(0.1776)$
DF	$1^3A_g^+$	3.59	0.0	$ H \rightarrow L + 3\rangle + c.c.(0.5042)$ $ H - 1 \rightarrow L + 2\rangle + c.c.(0.2449)$
I	$1^3B_{1g}^-$	4.57	1.394	$ H \rightarrow L + 2\rangle + c.c.(0.6219)$ $ H \rightarrow L; H - 1 \rightarrow L\rangle + c.c.(0.0854)$
II	$1^3A_g^-$	5.44	0.521	$ H \rightarrow L + 3\rangle - c.c.(0.5463)$ $ H - 1 \rightarrow L + 2\rangle - c.c.(0.2938)$
III	$2^3A_g^-$	5.72	0.370	$ H - 1 \rightarrow L + 2\rangle - c.c.(0.5371)$ $ H \rightarrow L + 3\rangle - c.c.(0.2765)$
IV	$2^3B_{1g}^-$	6.29	1.335	$ H \rightarrow L; H \rightarrow L + 1\rangle + c.c.(0.5577)$ $ H - 1 \rightarrow L + 3\rangle + c.c.(0.2127)$
V	$3^3B_{1g}^-$	6.78	0.544	$ H - 1 \rightarrow L + 3\rangle + c.c.(0.5194)$ $ H \rightarrow L; H \rightarrow L + 1\rangle + c.c.(0.1673)$
VI	$4^3A_g^-$	7.36	0.530	$ H \rightarrow L; H - 1 \rightarrow L + 1\rangle (0.5641)$ $ H \rightarrow L; H - 2 \rightarrow L + 2\rangle (0.4119)$
	$5^3A_g^-$	7.40	0.387	$ H \rightarrow L; H - 2 \rightarrow L + 2\rangle (0.6385)$ $ H \rightarrow L + 6\rangle - c.c.(0.3256)$
VII	$6^3A_g^-$	7.64	0.652	$ H \rightarrow L; H - 1 \rightarrow L + 1\rangle (0.7058)$ $ H - 3 \rightarrow L + 4\rangle + c.c.(0.2388)$

Table IX. Properties of the excited states leading to various peaks in the triplet absorption spectrum of tetracene computed using the MRSDCI method, and the standard parameters in the PPP model Hamiltonian. The rest of the information is same as in the caption of Table V.

Peak	State	E (eV)	Transition Dipole ( $\text{\AA}$ )	Dominant Contributing Configurations
DF	$1^3B_{1g}^+$	2.34	0.0	$ H \rightarrow L + 1\rangle - c.c.(0.5959)$ $ H - 1 \rightarrow L + 3\rangle + c.c.(0.1194)$
DF	$1^3A_g^+$	3.80	0.0	$ H \rightarrow L + 4\rangle - c.c.(0.4892)$ $ H - 1 \rightarrow L + 2\rangle + c.c.(0.3127)$
I	$1^3B_{1g}^-$	4.30	1.501	$ H \rightarrow L + 1\rangle + c.c.(0.5876)$ $ H \rightarrow L; H \rightarrow L + 2\rangle + c.c.(0.1630)$
II	$1^3A_g^-$	5.07	0.356	$ H - 1 \rightarrow L + 2\rangle - c.c.(0.4523)$ $ H \rightarrow L + 4\rangle + c.c.(0.4234)$
III	$3^3B_{1g}^-$	6.23	1.865	$ H \rightarrow L; H \rightarrow L + 2\rangle + c.c.(0.5446)$ $ H - 1 \rightarrow L; H \rightarrow L + 4\rangle c.c.(0.1402)$
IV	$3^3A_g^-$	6.59	0.346	$ H \rightarrow L; H - 1 \rightarrow L + 1\rangle (0.4758)$ $ H \rightarrow L; H \rightarrow L + 3\rangle + c.c.(0.4152)$
	$4^3A_g^-$	6.64	0.654	$ H \rightarrow L; H - 1 \rightarrow L + 1\rangle (0.6786)$ $ H \rightarrow L + 4\rangle + c.c.(0.1947)$
V	$6^3A_g^-$	7.39	0.239	$ H \rightarrow L; H - 1 \rightarrow L + 1\rangle (0.4877)$ $ H \rightarrow L; H - 2 \rightarrow L + 2\rangle (0.3882)$

Table X. Properties of the excited states leading to various peaks in the triplet absorption spectrum of tetracene computed using the MRSDCI method, and the screened parameters in the PPP model Hamiltonian. The rest of the information is same as in the caption of Table V.

Peak	State	E (eV)	Transition Dipole ( $\text{\AA}$ )	Dominant Contributing Configurations
DF	$1^3B_{1g}^+$	2.15	0.0	$ H \rightarrow L + 1\rangle + c.c.(0.5828)$ $ H - 1 \rightarrow L + 3\rangle + c.c.(0.1199)$
DF	$1^3A_g^+$	3.53	0.0	$ H \rightarrow L + 4\rangle - c.c.(0.5092)$ $ H - 1 \rightarrow L + 2\rangle - c.c.(0.2542)$
I	$1^3B_{1g}^-$	3.90	1.824	$ H \rightarrow L + 1\rangle - c.c.(0.6176)$ $ H \rightarrow L + 1; H - 1 \rightarrow L + 2\rangle c.c.(0.0735)$
II	$1^3A_g^-$	5.02	0.524	$ H \rightarrow L + 4\rangle + c.c.(0.5638)$ $ H - 1 \rightarrow L + 2\rangle + c.c.(0.2617)$
III	$3^3B_{1g}^-$	5.78	1.648	$ H \rightarrow L; H \rightarrow L + 2\rangle + c.c.(0.5793)$ $ H - 1 \rightarrow L; H - 2 \rightarrow L + 1\rangle c.c.(0.1355)$
IV	$4^3B_{1g}^-$	6.28	0.203	$ H - 1 \rightarrow L + 3\rangle - c.c.(0.5696)$ $ H \rightarrow L; H \rightarrow L; H - 1 \rightarrow L + 3\rangle - c.c.(0.1273)$
	$3^3A_g^-$	6.31	0.779	$ H \rightarrow L; H - 1 \rightarrow L + 1\rangle (0.8320)$ $ H \rightarrow L + 1; H - 1 \rightarrow L + 3\rangle - c.c.(0.1013)$
V	$7^3B_{1g}^-$	7.33	0.503	$ H \rightarrow L; H - 2 \rightarrow L + 3\rangle - c.c.(0.3526)$ $ H \rightarrow L + 1; H - 4 \rightarrow L\rangle - c.c.(0.3303)$
	$8^3A_g^-$	7.42	0.785	$ H \rightarrow L; H - 2 \rightarrow L + 2\rangle (0.7912)$ $ H - 1 \rightarrow L + 2; H - 2 \rightarrow L + 1\rangle (0.1316)$



Table XI. Properties of the excited states leading to various peaks in the triplet absorption spectrum of pentacene computed using the MRSDCI method, and the standard parameters in the PPP model Hamiltonian. The rest of the information is same as in the caption of Table V.

Peak	State	E (eV)	Transition Dipole (Å)	Dominant Contributing Configurations
DF	$1^3B_{1g}^+$	1.95	0.0	$ H \rightarrow L + 1\rangle - c.c.(0.5890)$ $ H - 1 \rightarrow L + 3\rangle - c.c.(0.1143)$
DF	$1^3A_g^+$	3.66	0.0	$ H \rightarrow L + 4\rangle - c.c.(0.4589)$ $ H - 1 \rightarrow L + 2\rangle + c.c.(0.3251)$
I	$1^3B_{1g}^-$	3.86	1.842	$ H \rightarrow L + 1\rangle + c.c.(0.5785)$ $ H \rightarrow L; H \rightarrow L + 2\rangle + c.c.(0.1413)$
II	$1^3A_g^-$	4.76	0.303	$ H - 1 \rightarrow L + 2\rangle - c.c.(0.4328)$ $ H \rightarrow L + 4\rangle + c.c.(0.4179)$
III	$3^3B_{1g}^-$	5.84	2.02	$ H \rightarrow L; H \rightarrow L + 2\rangle + c.c.(0.5287)$ $ H - 1 \rightarrow L; H \rightarrow L + 4\rangle c.c.(0.1615)$
IV	$3^3A_g^-$	6.09	0.373	$ H \rightarrow L; H - 1 \rightarrow L + 1\rangle (0.5984)$ $ H \rightarrow L; H \rightarrow L + 3\rangle - c.c.(0.3464)$
	$4^3A_g^-$	6.15	0.706	$ H \rightarrow L; H - 1 \rightarrow L + 1\rangle (0.3977)$ $ H \rightarrow L + 4\rangle + c.c.(0.3550)$
V	$6^3B_{1g}^-$	7.15	0.669	$ H \rightarrow L + 1; H - 4 \rightarrow L\rangle - c.c.(0.3978)$ $ H - 1 \rightarrow L + 2; H \rightarrow L + 1\rangle - c.c.(0.2217)$

Table XII. Properties of the excited states leading to various peaks in the triplet absorption spectrum of pentacene computed using the MRSDCI method, and the screened parameters in the PPP model Hamiltonian. The rest of the information is same as in the caption of Table V.

Peak	State	E (eV)	Transition Dipole ( $\text{\AA}$ )	Dominant Contributing Configurations
DF	$1^3B_{1g}^+$	1.83	0.0	$ H \rightarrow L + 1\rangle - c.c.(0.5815)$ $ H - 1 \rightarrow L + 3\rangle - c.c.(0.1207)$
DF	$1^3A_g^+$	3.37	0.0	$ H \rightarrow L + 4\rangle + c.c.(0.4773)$ $ H - 1 \rightarrow L + 2\rangle - c.c.(0.2856)$
I	$1^3B_{1g}^-$	3.47	2.208	$ H \rightarrow L + 1\rangle + c.c.(0.6091)$ $ H - 1 \rightarrow L + 3\rangle + c.c.(0.0766)$
II	$1^3A_g^-$	4.72	0.396	$ H \rightarrow L + 4\rangle - c.c.(0.5163)$ $ H - 1 \rightarrow L + 2\rangle + c.c.(0.3126)$
III	$3^3B_{1g}^-$	5.51	1.816	$ H \rightarrow L; H \rightarrow L + 2\rangle + c.c.(0.5701)$ $ H - 1 \rightarrow L; H - 2 \rightarrow L + 1\rangle c.c.(0.1440)$
IV	$5^3B_{1g}^-$	6.78	0.743	$ H \rightarrow L + 1; H - 4 \rightarrow L\rangle - c.c.(0.3970)$ $ H \rightarrow L + 1; H - 1 \rightarrow L + 2\rangle - c.c.(0.2538)$
V	$11^3A_g^-$	7.33	0.805	$ H \rightarrow L; H - 2 \rightarrow L + 2\rangle (0.7543)$ $ H - 1 \rightarrow L + 7\rangle + c.c.(0.1390)$
	$12^3A_g^-$	7.35	0.334	$ H \rightarrow L + 3; H - 1 \rightarrow L + 1\rangle - c.c.(0.3503)$ $ H \rightarrow L; H - 1 \rightarrow L + 5\rangle - c.c.(0.3135)$

Table XIII. Properties of the excited states leading to various peaks in the triplet absorption spectrum of hexacene computed using the MRSDCI method, and the standard parameters in the PPP model Hamiltonian. The rest of the information is same as in the caption of Table V.

Peak	State	E (eV)	Transition Dipole (Å)	Dominant Contributing Configurations
DF	$1^3B_{1g}^+$	1.67	0.0	$ H \rightarrow L + 1\rangle + c.c.(0.5841)$ $ H - 1 \rightarrow L + 2\rangle + c.c.(0.1239)$
DF	$1^3A_g^+$	3.50	0.0	$ H \rightarrow L + 4\rangle - c.c.(0.4127)$ $ H - 1 \rightarrow L + 3\rangle + c.c.(0.3077)$
I	$1^3B_{1g}^-$	3.57	2.153	$ H \rightarrow L + 1\rangle - c.c.(0.5705)$ $ H - 1 \rightarrow L + 2\rangle - c.c.(0.1471)$
	$1^3A_g^-$	4.61	0.218	$ H - 1 \rightarrow L + 3\rangle + c.c.(0.4363)$ $ H \rightarrow L + 4\rangle + c.c.(0.4341)$
II	$2^3A_g^-$	5.15	0.647	$ H \rightarrow L; H - 1 \rightarrow L + 1\rangle (0.8093)$ $ H \rightarrow L; H - 3 \rightarrow L + 3\rangle (0.1337)$
III	$3^3B_{1g}^-$	5.62	2.119	$ H \rightarrow L; H \rightarrow L + 3\rangle - c.c.(0.5159)$ $ H \rightarrow L + 1; H - 4 \rightarrow L\rangle c.c.(0.1642)$
IV	$4^3A_g^-$	5.98	0.482	$ H \rightarrow L + 4\rangle + c.c.(0.3650)$ $ H - 1 \rightarrow L + 3\rangle - c.c.(0.3138)$
	$4^3B_{1g}^-$	5.98	0.380	$ H - 1 \rightarrow L + 2\rangle - c.c.(0.4471)$ $ H \rightarrow L + 1; H - 1 \rightarrow L + 3\rangle - c.c.(0.2035)$
V	$7^3B_{1g}^-$	6.82	1.056	$ H \rightarrow L + 1; H - 4 \rightarrow L\rangle - c.c.(0.4144)$ $ H \rightarrow L + 1; H - 1 \rightarrow L + 3\rangle - c.c.(0.2725)$

Table XIV. Properties of the excited states leading to various peaks in the triplet absorption spectrum of hexacene computed using the MRSDCI method, and the screened parameters in the PPP model Hamiltonian. The rest of the information is same as in the caption of Table V.

Peak	State	E (eV)	Transition Dipole (Å)	Dominant Contributing Configurations
DF	$1^3B_{1g}^+$	1.60	0.0	$ H \rightarrow L + 1\rangle + c.c.(0.5799)$ $ H - 1 \rightarrow L + 2\rangle + c.c.(0.1197)$
DF	$1^3A_g^+$	3.10	0.0	$ H \rightarrow L + 4\rangle + c.c.(0.4573)$ $ H - 1 \rightarrow L + 3\rangle + c.c.(0.2732)$
I	$1^3B_{1g}^-$	3.18	2.485	$ H \rightarrow L + 1\rangle - c.c.(0.6018)$ $ H - 1 \rightarrow L + 2\rangle - c.c.(0.0854)$
	$1^3A_g^-$	4.50	0.191	$ H \rightarrow L; H - 1 \rightarrow L + 1\rangle (0.6134)$ $ H \rightarrow L; H \rightarrow L + 2\rangle + c.c.(0.3260)$
II	$2^3A_g^-$	4.85	0.715	$ H \rightarrow L; H - 1 \rightarrow L + 1\rangle (0.5609)$ $ H \rightarrow L + 4\rangle - c.c.(0.3636)$
	$2^3B_{1g}^-$	4.88	0.435	$ H \rightarrow L + 5\rangle + c.c.(0.5435)$ $ H - 2 \rightarrow L + 1\rangle - c.c.(0.2464)$
III	$4^3B_{1g}^-$	5.17	1.776	$ H \rightarrow L; H \rightarrow L + 3\rangle - c.c.(0.5398)$ $ H - 2 \rightarrow L + 1\rangle - c.c.(0.1420)$
IV	$5^3B_{1g}^-$	6.23	1.114	$ H \rightarrow L; H \rightarrow L + 3\rangle - c.c.(0.5398)$ $ H - 2 \rightarrow L + 1\rangle - c.c.(0.1420)$
	$5^3A_g^-$	6.26	0.139	$ H \rightarrow L; H - 1 \rightarrow L + 5\rangle - c.c.(0.3769)$ $ H \rightarrow L + 1; H - 2 \rightarrow L + 1\rangle - c.c.(0.3675)$
V	$10^3A_g^-$	6.77	0.159	$ H \rightarrow L + 2; H - 1 \rightarrow L + 1\rangle - c.c.(0.4111)$ $ H \rightarrow L; H \rightarrow L + 2\rangle - c.c.(0.2945)$
	$11^3B_{1g}^-$	6.85	0.441	$ H \rightarrow L; H \rightarrow L + 7\rangle + c.c.(0.2565)$ $ H - 2 \rightarrow L + 5\rangle + c.c.(0.2555)$

Table XV. Properties of the excited states leading to various peaks in the triplet absorption spectrum of heptacene computed using the MRSDCI method, and the standard parameters in the PPP model Hamiltonian. The rest of the information is same as in the caption of Table V.

Peak	State	E (eV)	Transition Dipole ( $\text{\AA}$ )	Dominant Contributing Configurations
DF	$1^3B_{1g}^+$	1.42	0	$ H \rightarrow L + 1\rangle + c.c.(0.5809)$ $ H \rightarrow L + 4\rangle + c.c.(0.1313)$
DF	$1^3A_g^+$	3.07	0	$ H \rightarrow L; H - 1 \rightarrow L + 1\rangle (0.4476)$ $ H \rightarrow L + 5\rangle - c.c.(0.2726)$
I	$1^3B_{1g}^-$	3.31	2.411	$ H \rightarrow L + 1\rangle - c.c.(0.5652)$ $ H - 1 \rightarrow L + 2\rangle - c.c.(0.1612)$
II	$1^3A_g^-$	4.45	0.438	$ H \rightarrow L; H - 1 \rightarrow L + 1\rangle (0.6770)$ $ H \rightarrow L + 5\rangle + c.c.(0.2778)$
	$2^3A_g^-$	4.58	0.627	$ H \rightarrow L; H - 1 \rightarrow L + 1\rangle (0.5450)$ $ H - 1 \rightarrow L + 3\rangle - c.c.(0.3565)$
III	$3^3B_{1g}^-$	5.46	2.368	$ H \rightarrow L; H \rightarrow L + 3\rangle - c.c.(0.5201)$ $ H \rightarrow L + 1; H - 5 \rightarrow L\rangle c.c.(0.1864)$
IV	$9^3A_g^-$	6.48	0.314	$ H \rightarrow L + 2; H - 1 \rightarrow L + 1\rangle - c.c.(0.3296)$ $ H \rightarrow L; H - 1 \rightarrow L + 4\rangle - c.c.(0.2959)$
	$6^3B_{1g}^-$	6.51	1.142	$ H \rightarrow L + 1; H - 5 \rightarrow L\rangle c.c.(0.4693)$ $ H \rightarrow L + 1; H - 1 \rightarrow L + 3\rangle c.c.(0.3070)$

Table XVI. Properties of the excited states leading to various peaks in the triplet absorption spectrum of heptacene computed using the MRSDCI method, and the screened parameters in the PPP model Hamiltonian. The rest of the information is same as in the caption of Table V.

Peak	State	E (eV)	Transition Dipole ( $\text{\AA}$ )	Dominant Contributing Configurations
DF	$1^3B_{1g}^+$	1.30	0.0	$ H \rightarrow L + 1\rangle + c.c.(0.5728)$ $ H - 1 \rightarrow L + 2\rangle + c.c.(0.1278)$
DF	$1^3A_g^+$	2.59	0.0	$ H \rightarrow L; H - 1 \rightarrow L + 1\rangle (0.7028)$ $ H \rightarrow L + 2; H - 1 \rightarrow L + 1\rangle - c.c.(0.2562)$
I	$1^3B_{1g}^-$	2.83	2.708	$ H \rightarrow L + 1\rangle - c.c.(0.5973)$ $ H - 1 \rightarrow L + 2\rangle - c.c.(0.0932)$
II	$1^3A_g^-$	3.84	0.756	$ H \rightarrow L; H - 1 \rightarrow L + 1\rangle (0.8354)$ $ H \rightarrow L + 2; H - 1 \rightarrow L + 1\rangle - c.c.(0.1082)$
III	$2^3A_g^-$	4.28	0.157	$ H \rightarrow L; H - 1 \rightarrow L + 1\rangle (0.7992)$ $ H - 1 \rightarrow L + 1; H - 2 \rightarrow L\rangle c.c.(0.1401)$
	$2^3B_{1g}^-$	4.28	0.624	$ H \rightarrow L + 4\rangle + c.c.(0.4639)$ $ H - 1 \rightarrow L + 2\rangle - c.c.(3640)$
IV	$3^3A_g^-$	4.49	0.614	$ H \rightarrow L + 5\rangle + c.c.(0.5809)$ $ H - 1 \rightarrow L; H - 1 \rightarrow L + 1\rangle (0.1796)$
	$3^3B_{1g}^-$	4.45	0.519	$ H - 1 \rightarrow L + 2\rangle - c.c.(0.4166)$ $ H \rightarrow L + 4\rangle + c.c.(3838)$
V	$4^3B_{1g}^-$	4.8	2.177	$ H \rightarrow L; H \rightarrow L + 3\rangle - c.c.(0.5665)$ $ H \rightarrow L + 1; H - 1 \rightarrow L + 3\rangle c.c.(0.1631)$
VI	$5^3B_{1g}^-$	5.63	1.361	$ H \rightarrow L + 1; H - 5 \rightarrow L\rangle - c.c.(0.5143)$ $ H \rightarrow L + 1; H - 1 \rightarrow L + 3\rangle - c.c.(0.2377)$
VII	$8^3B_{1g}^-$	6.11	0.508	$ H - 2 \rightarrow L + 4\rangle + c.c.(0.3988)$ $ H \rightarrow L + 1; H - 5 \rightarrow L\rangle - c.c.(0.3343)$
	$11^3A_g^-$	6.17	0.299	$ H \rightarrow L; H - 1 \rightarrow L + 4\rangle - c.c.(0.3075)$ $ H \rightarrow L + 2; H - 1 \rightarrow L + 1\rangle - c.c.(0.3065)$

- 
- [1] A. Skotheim and J. E. Reynolds, *Conjugated Polymers: Theory, Synthesis, Properties, and Characterization* (CRC Press, 2006).
- [2] K. Müllen and G. Wegner, *Electronic materials: the oligomer approach* (Wiley-VCH, 1998).
- [3] W. Barford, *Electronic and Optical Properties of Conjugated Polymers* (Oxford University Press, 2005).
- [4] M. B. Smith and J. Michl, *Chemical Reviews* **110**, 6891 (2010).
- [5] M. B. Smith and J. Michl, *Annual Review of Physical Chemistry* **64**, 361 (2013), pMID: 23298243, <http://dx.doi.org/10.1146/annurev-physchem-040412-110130>.
- [6] A. Shukla, *Phys. Rev. B* **65**, 125204 (2002).
- [7] M. Bendikov, F. Wudl, and D. F. Perepichka, *Chem. Rev.* **104**, 4891 (2004).
- [8] J. E. Anthony, *Chem. Rev.* **106**, 5028 (2006).
- [9] A. Bjørseth, *Handbook of polycyclic aromatic hydrocarbons*, v. 1 (Dekker, 1983).
- [10] R. Harvey, *Polycyclic Aromatic Hydrocarbons: Chemistry and Carcinogenicity* (Cambridge University Press, 1991).
- [11] J. E. Anthony, *Angew. Chem. Int. Ed.* **47**, 452 (2008).
- [12] R. Mondal, A. N. Okhrimenko, B. K. Shah, and D. C. Neckers, *J. Phys. Chem. B* **112**, 11 (2008), pMID: 18069818.
- [13] R. Mondal, C. Tönshoff, D. Khon, D. C. Neckers, and H. F. Bettinger, *J. Am. Chem. Soc.* **131**, 14281 (2009).
- [14] I. Kaur, M. Jazdyk, N. N. Stein, P. Prusevich, and G. P. Miller, *J. Am. Chem. Soc.* **132**, 1261 (2010).
- [15] C. Tönshoff and H. Bettinger, *Angew. Chem. Int. Ed.* **49**, 4125 (2010).
- [16] P. Sony and A. Shukla, *Phys. Rev. B* **75**, 155208 (2007).
- [17] G. N. Lewis and M. Kasha, *J. Am. Chem. Soc.* **66**, 2100 (1944).
- [18] D. S. McClure, *J. Chem. Phys.* **17**, 905 (1949).
- [19] H. Hunziker, *Chem. Phys. Lett.* **3**, 504 (1969).
- [20] H. E. Hunziker, *J. Chem. Phys.* **56**, 400 (1972).

- [21] Y. H. Meyer, R. Astier, and J. M. Leclercq, *J. Chem. Phys.* **56**, 801 (1972).
- [22] S. P. McGlynn, T. Azumi, and M. Kasha, *J. Chem. Phys.* **40**, 507 (1964).
- [23] G. Porter and F. J. Wright, *Trans. Faraday Soc.* **51**, 1205 (1955).
- [24] M. Allan, *J. Electron Spectrosc. Relat. Phenom.* **48**, 219 (1989).
- [25] N. Sabbatini, M. T. Indelli, M. T. Gandolfi, and V. Balzani, *J. Phys. Chem.* **86**, 3585 (1982).
- [26] G. Porter and M. W. Windsor, *Proc. Roy. Soc. A* **245**, 238 (1958).
- [27] T. G. Pavlopoulos, *J. Chem. Phys.* **56**, 227 (1972).
- [28] J. Burgos, M. Pope, C. E. Swenberg, and R. R. Alfano, *Phys. Status Solidi B* **83**, 249 (1977).
- [29] C. Hellner, L. Lindqvist, and P. C. Roberge, *J. Chem. Soc., Faraday Trans. 2* **68**, 1928 (1972).
- [30] H. Angliker, E. Rommel, and J. Wirz, *Chem. Phys. Lett.* **87**, 208 (1982).
- [31] J. J. Burdett and C. J. Bardeen, *Acc. Chem. Res.* **46**, 1312 (2013).
- [32] V. K. Thorsmølle, R. D. Averitt, J. Demsar, D. L. Smith, S. Tretiak, R. L. Martin, X. Chi, B. K. Crone, A. P. Ramirez, and A. J. Taylor, *Phys. Rev. Lett.* **102**, 017401 (2009).
- [33] F. Anger, J. O. Ossó, U. Heinemeyer, K. Broch, R. Scholz, A. Gerlach, and F. Schreiber, *J. Chem. Phys.* **136**, 054701 (2012).
- [34] A. Rao, M. W. B. Wilson, J. M. Hodgkiss, S. Albert-Seifried, H. Bässler, and R. H. Friend, *J. Am. Chem. Soc.* **132**, 12698 (2010).
- [35] M. Muntwiler, Q. Yang, and X.-Y. Zhu, *J. Electron Spectrosc. and Rel. Phenom.* **174**, 116 (2009), advanced Spectroscopies of Molecular Materials for Electronics.
- [36] H. Marciniak, I. Pugliesi, B. Nickel, and S. Lochbrunner, *Phys. Rev. B* **79**, 235318 (2009).
- [37] C. Jundt, G. Klein, B. Sipp, J. L. Moigne, M. Joucla, and A. Villaeys, *Chem. Phys. Lett.* **241**, 84 (1995).
- [38] J. A. Pople, *Trans. Faraday Soc.* **49**, 1375 (1953).
- [39] R. Pariser and R. G. Parr, *J. Chem. Phys.* **21**, 767 (1953).
- [40] R. Pariser, *J. Chem. Phys.* **24**, 250 (1956).
- [41] R. L. de Groot and G. J. Hoytink, *J. Chem. Phys.* **46**, 4523 (1967).
- [42] M. Baldo, A. Grassi, R. Pucci, and P. Tomasello, *J. Chem. Phys.* **77**, 2438 (1982).
- [43] C. Raghu, Y. Anusooya Pati, and S. Ramasesha, *Phys. Rev. B* **66**, 035116 (2002).
- [44] Y. A. Pati and S. Ramasesha, *J. Phys. Chem. A* **118**, 4048 (2014), <http://pubs.acs.org/doi/pdf/10.1021/jp502813w>.
- [45] N. O. Lipari and C. B. Duke, *J. Chem. Phys.* **63**, 1768 (1975).



- [46] P. Swiderek, M. Michaud, G. Hohlneicher, and L. Sanche, *Chem. Phys. Lett.* **175**, 667 (1990).
- [47] Y. Gao, C.-G. Liu, and Y.-S. Jiang, *J. Phys. Chem. A* **106**, 2592 (2002).
- [48] M. Rubio, M. Merchán, E. Ortí, and B. O. Roos, *Chem. Phys.* **179**, 395 (1994).
- [49] T. Hashimoto, H. Nakano, and K. Hirao, *J. Chem. Phys.* **104**, 6244 (1996).
- [50] Y. Kawashima, T. Hashimoto, H. Nakano, and K. Hirao, *Theor. Chem. Acc.* **102**, 49 (1999).
- [51] P. M. Zimmerman, Z. Zhang, and C. B. Musgrave, *Nat Chem* **2**, 648 (2010).
- [52] J. Hachmann, J. J. Dorando, M. Aviles, and G. K.-L. Chan, *J. Chem. Phys.* **127**, 134309 (2007).
- [53] B. Hajgató, D. Szieberth, P. Geerlings, F. De Proft, and M. S. Deleuze, *J. Chem. Phys.* **131**, 224321 (2009).
- [54] K. N. Houk, P. S. Lee, and M. Nendel, *J. Org. Chem.* **66**, 5517 (2001).
- [55] C. Quarti, D. Fazzi, and M. Del Zoppo, *Phys. Chem. Chem. Phys.* **13**, 18615 (2011).
- [56] K. Hummer and C. Ambrosch-Draxl, *Phys. Rev. B* **71**, 081202 (2005).
- [57] K. A. Nguyen, J. Kennel, and R. Pachter, *J. Chem. Phys.* **117**, 7128 (2002).
- [58] D.-e. Jiang and S. Dai, *J. Phys. Chem. A* **112**, 332 (2008).
- [59] H. Chakraborty and A. Shukla, *J. Phys. Chem. A* **117**, 14220 (2013).
- [60] K. Ohno, *Theor. Chim. Acta* **2**, 219 (1964).
- [61] M. Chandross and S. Mazumdar, *Phys. Rev. B* **55**, 1497 (1997).
- [62] M. Bendikov, H. M. Duong, K. Starkey, K. N. Houk, E. A. Carter, and F. Wudl, *J. Am. Chem. Soc.* **126**, 7416 (2004).
- [63] M. Huzak, M. S. Deleuze, and B. Hajgató, *J. Chem. Phys.* **135**, 104704 (2011).
- [64] B. Hajgató and M. S. Deleuze, *Chem. Phys. Lett.* **553**, 6 (2012).
- [65] P. Sony and A. Shukla, *Comput. Phys. Commun.* **181**, 821 (2010).
- [66] R. J. Buenker, S. D. Peyerimhoff, and W. Butscher, *Mol. Phys.* **35**, 771 (1978).
- [67] R. Buenker and S. Peyerimhoff, *Theor. Chim. Acta* **35**, 33 (1974).
- [68] A. Shukla, *Phys. Rev. B* **69**, 165218 (2004).
- [69] A. Shukla, *Chem. Phys.* **300**, 177 (2004).
- [70] H. Ghosh, A. Shukla, and S. Mazumdar, *Phys. Rev. B* **62**, 12763 (2000).
- [71] L. E. McMurchie, S. T. Elbert, S. R. Langhoff, and E. R. Davidson, MELD package from Indiana University. It has been modified by us to handle bigger systems.

- [72] M. Schreiber, M. R. Silva-Junior, S. P. A. Sauer, and W. Thiel, *J. Chem. Phys.* **128**, 134110 (2008).
- [73] S. Ramasesha and Z. Soos, *Chem. Phys.* **91**, 35 (1984).
- [74] J. Schiedt and R. Weinkauff, *Chem. Phys. Lett.* **266**, 201 (1997).
- [75] Y. Tomkiewicz, R. P. Groff, and P. Avakian, *J. Chem. Phys.* **54**, 4504 (1971).
- [76] G. G. Hall, *Proc. Roy. Soc. A* **213**, 113 (1952).
- [77] N. Nijegorodov, V. Ramachandran, and D. Winkoun, *Spectrochim. Acta Part A* **53**, 1813 (1997).
- [78] S. Ramasesha, D. S. Galvao, and Z. G. Soos, *J. Phys. Chem.* **97**, 2823 (1993), <http://pubs.acs.org/doi/pdf/10.1021/j100114a002>.
- [79] Y. Shimoi and S. Mazumdar, *Synthetic Metals* **85**, 1027 (1997).
- [80] P. Sony and A. Shukla, *J. Chem. Phys.* **131**, 014302 (2009).
- [81] C. Raghu, Y. A. Pati, and S. Ramasesha, *Phys. Rev. B* **65**, 155204 (2002).